THE UNIVERSITY OF MICHIGAN

INDUSTRY PROGRAM OF THE COLLEGE OF ENGINEERING

EARTHQUAKE RESPONSE OF A RAMBERG-OSGOOD STRUCTURE

Movses J. Kaldjian
William R. S. Fan

December, 1967

IP-802

ACKNOWLEDGMENTS

This report was prepared for a research project "Response of Steel Frame Structures to Earthquake Motion," conducted at the University of Michigan under the sponsorships of the American Iron and Steel Institute.

The writers are deeply indebted to Glen V. Berg, director of the project, for his valuable assistance and helpful suggestions. The assistance and advice of Robert D. Hanson who reviewed this report, is also gratefully acknowledged.

TABLE OF CONTENTS

LIST OF FIGURES

INTRODUCTION

It would be an ideal situation if the designer of an earthquake-resistant frame structure could know the response of the structure to the ground motion to which it would be subjected in its useful lifetime. This response is not possible to obtain. The nature of the ground motion encountered in earthquakes and the type of structures the engineer has to work with are much too complicated for that. On the other hand, much can be learned about structural behavior in earthquakes by response spectrum analyses of past strong-motion earthquakes. Moreover, the response spectrum is a powerful tool to aid the designer of earthquake-resistant structures. The general shape of the velocity response spectrum of an earthquake motion can also provide significant information about the expected inelastic response of a multi-story structure.(1)

Response spectrum analyses of strong-motion U. S. earthquakes(2) indicate seismic lateral forces to be much greater than the accepted code values currently in use in earthquake design, even when the structure is heavily damped. On the other hand, buildings designed in accordance with current seismic building codes have survived strong earthquakes without showing excessive structural damage. One possible explanation is that both the structural and nonstructural components remain active when strained beyond their elastic limits and the energy transmitted to the structure by the earthquake is dissipated by inelastic deformation. Dynamic response beyond the elastic range is therefore a topic worthy of further investigation.

The elasto-plastic load-displacement relation has been used in a great majority of the studies of inelastic response to earthquake. The present study includes the elasto-plastic relation as a special case of a more general load-displacement relation called the Ramberg-Osgood relation, (Reference 3) in which three parameters, a characteristic load, a characteristic displacement, and an exponent, characterize the behavior. Experimental work on structural steel members and connections[4] indicates that the Ramberg-Osgood relation is more realistic and can provide a better approximation of actual member behavior. The latter is also supported by analytical study.[5]

In this report the response of a single-degree-of-freedom structure subjected to strong motion earthquakes as well as to steady-state oscillations is studied. Effects of different earthquakes, and also various load-displacement shapes, i.e. degree of plasticity, on the response are some of the parameter considered. The principles and construction of the response spectra for Ramberg-Osgood systems are discussed in detail.

LOAD-DISPLACEMENT RELATIONS

Actual structural members do not exhibit ideal elasto-plastic load-displacement relations; rather, the load-displacement curve has an elastic branch followed by a transition curve that leads to a plastic branch. Upon reversed displacement, the Bauschinger effect makes the transition more gradual. This behavior can be represented quite closely by a relatively simple mathematical model, the Ramberg-Osgood function, shown in Figure 1. Three parameters are employed, a characteristic or yield load Q_y , a characteristic or yield displacement x_y , and an exponent r . It is the exponent r that governs the sharpness of the break away from the elastic branch. The Ramberg-Osgood function includes as special limiting cases the elastic case, obtained by setting $r = 1$, and the elasto-plastic case, obtained as r tends to infinity.

Some of the hysteresis loops obtained in recent tests of structural members and connections at the University of California[4] are shown in Figure 2 along with a Ramberg-Osgood loop with the parameters Q_y , x_y , and r chosen to give the best fit in the sense of least squares. Fitting the curve to experimental data requires too much computation to be done by hand, but with the aid of a computer the task is relatively simple. Curves have been fitted to other experimental load-displacement data, and it is found that the closeness of fit shown in Figure 2 is about typical. The Ramberg-Osgood representation of the load-displacement relation is considered realistic if the structure is capable of maintaining stable, nondeteriorating hysteresis loops.[6,7]

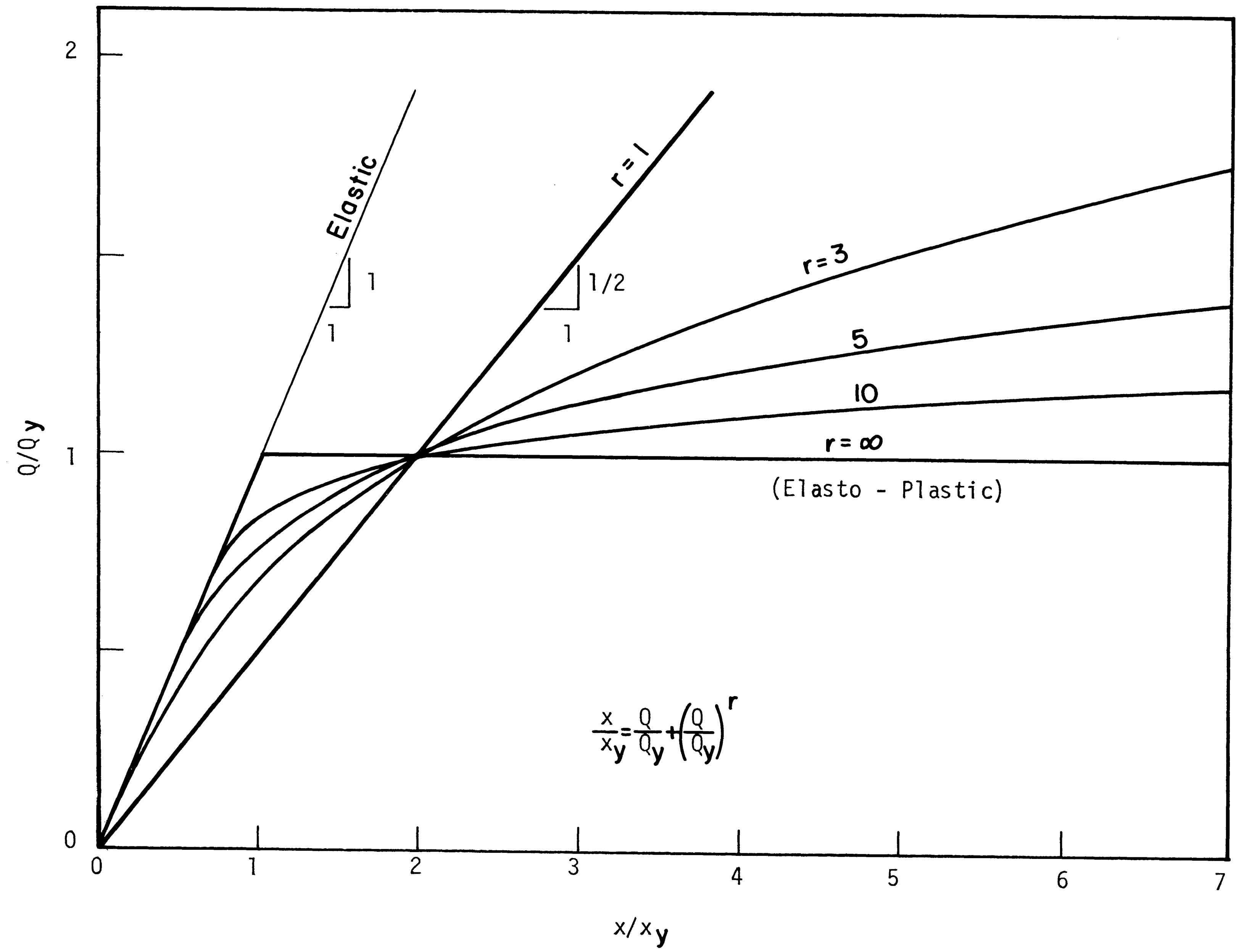

Figure 1. Ramberg-Osgood Functions.

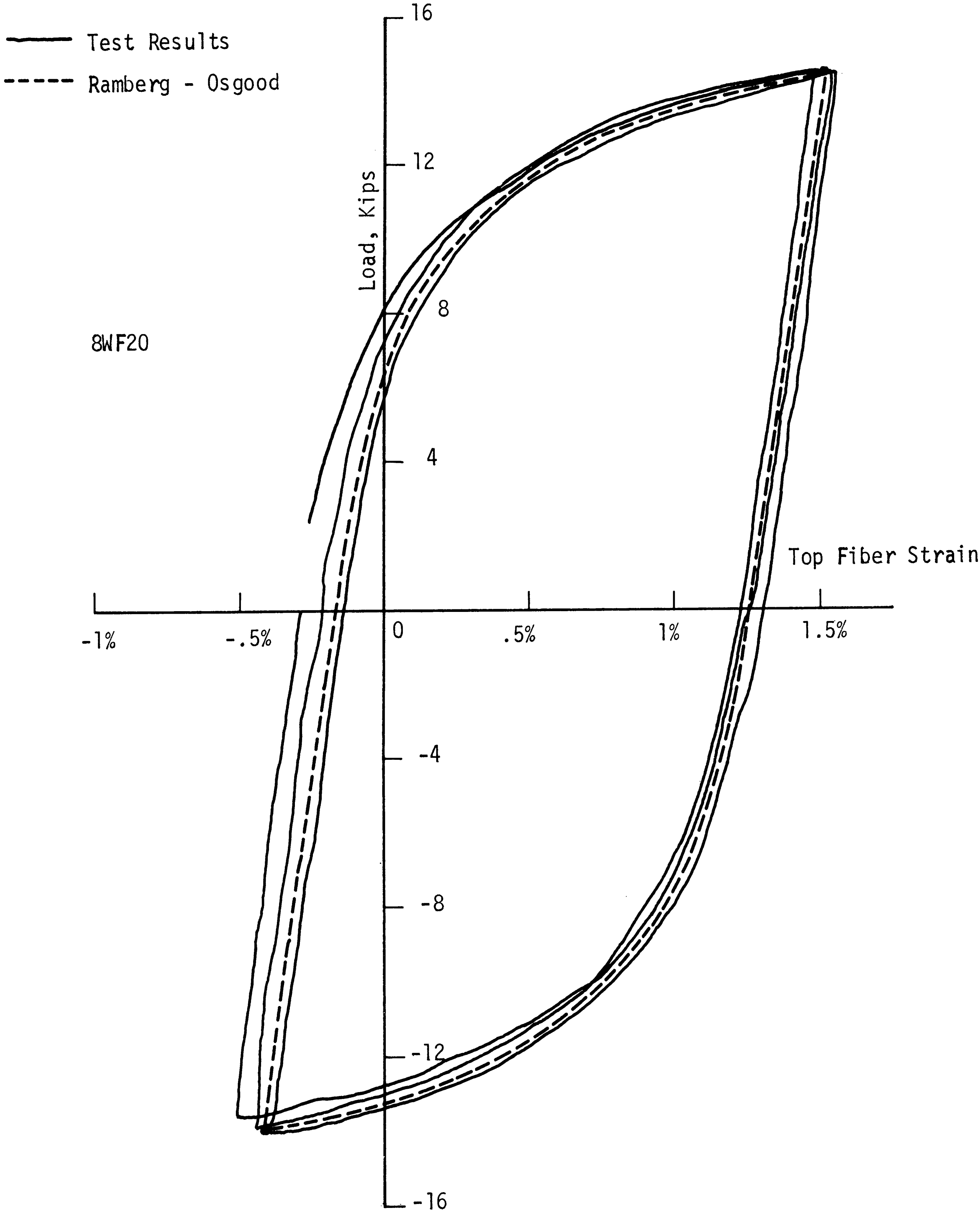

Figure 2. Experimental Hysteresis Loops.

THE DIFFERENTIAL EQUATION OF MOTION

A one-degree-of-freedom structure with Ramberg-Osgood characteristic can be represented by an equivalent oscillating system made of a single mass and a Ramberg-Osgood spring as shown in Figure 3.

The equation of motions for this system when subjected to ground motion is given by,

$$m(\ddot{x} + \ddot{y}) + Q = 0 \tag{1}$$

where

m = mass

x = relative displacement of mass to ground, a function of time

y = ground displacement, a function of time

Q = restoring force, a function of x

Differentiation with respect to time is denoted by dots. Rearranging and expressing in terms of unit mass this equation becomes,

$$\ddot{x} + q = - \ddot{y} \tag{2}$$

where

$$q = \frac{Q}{m}$$

The relation between the restoring force q and displacement x, see Figure 4, is given by,

$$\frac{x}{x_y} = \frac{q}{q_y}\left(1 + \left|\frac{q}{q_y}\right|^{r-1}\right) \tag{3}$$

where $q_y = Q_y/m$, is the characteristics restoring force per unit mass.

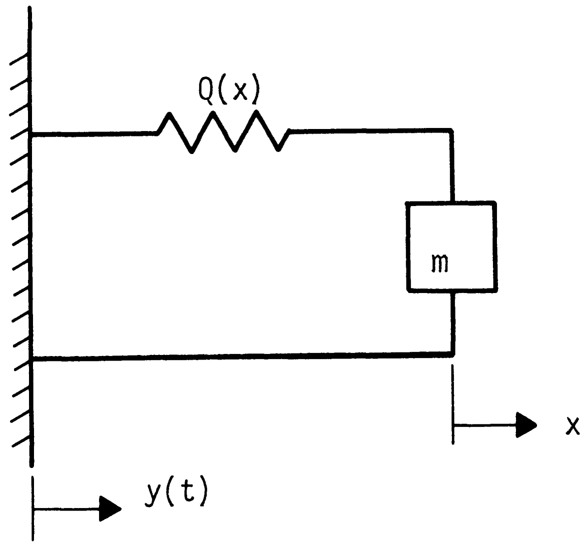

Figure 3. Equivalent Ramberg-Osgood System.

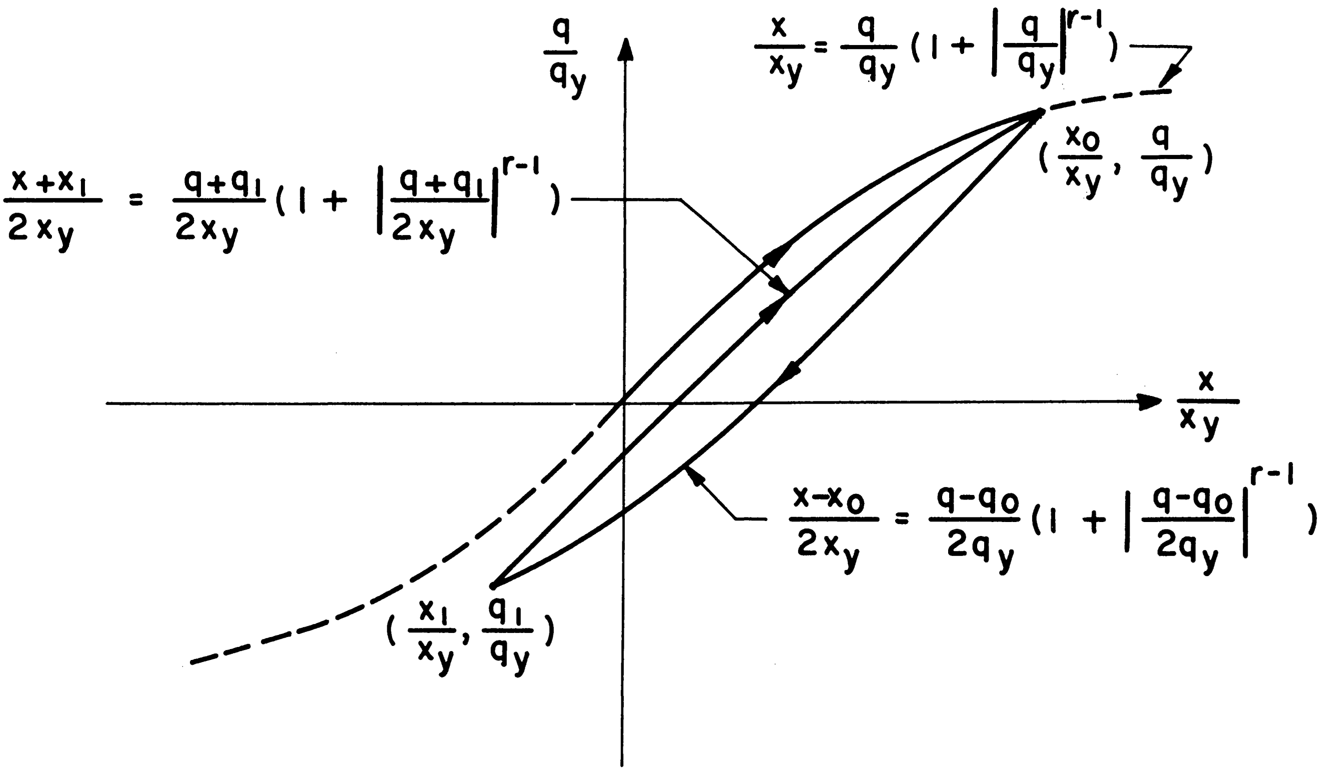

Figure 4. Ramberg-Osgood Load-Displacement Relations.

STEADY-STATE OSCILLATION

The dynamic response of actual structures to steady-state sinusoidal excitation can be obtained experimentally. Thus a study of the resonant amplitude, as a function of frequency and maximum amplitude of the forcing function would be useful in determining the Ramberg-Osgood parameters of real structures.[7]

The steady-state oscillation of a single-degree-of-freedom system with hysteretic force-displacement relation of the Ramberg-Osgood type, shown in Figure 5, has been studied both by the energy method[3] as well as by the method of slowly varying parameters.[3, 8] The energy method is limited in scope, for it gives the response at resonance only. The results of the slowly varying parameters method are considered in this section. The latter approach gives the steady-state response for all values of ω/ω_n i.e. forcing frequency to the undamped natural frequency, and can be used to plot amplitude against frequency curves.

In the absence of viscous damping, the equation of motion for this system is,

$$m\ddot{x} + Q(x) = F(t) = F_o \cos \omega t \qquad (4)$$

where F_o is the force amplitude and ω is the frequency of excitation.

The equation of motion, Equation (4), in dimensionless form becomes,

$$\frac{d^2}{d\tau^2}\left(\frac{x}{x_y}\right) + \frac{Q}{Q_y}\left(\frac{x}{x_y}\right) = \frac{F_o}{Q_y} \cos \eta t \qquad (5)$$

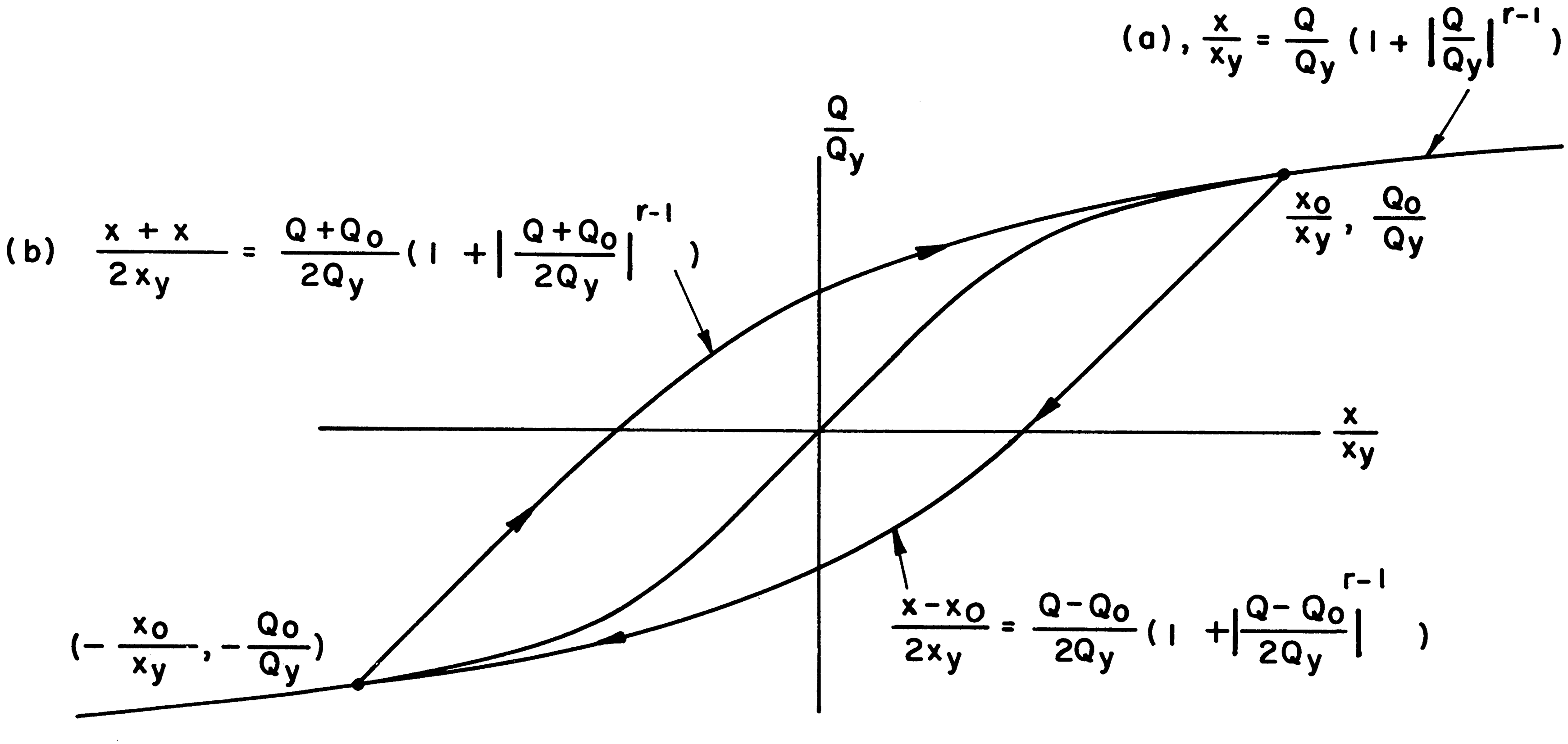

Figure 5. Ramberg-Osgood Hysteresis Loops.

where

$$\tau = \omega_n t$$

$$\eta = \frac{\omega}{\omega_n}$$

$$\frac{Q}{Q_y}\left(\frac{x}{x_y}\right) = Q(x)/Q_y$$

and

$$\omega_n = \sqrt{\frac{Q_y}{mx_y}}$$, the undamped natural frequency

Let the solution for Equation (5) be

$$\frac{x}{x_y} = \frac{x_o}{x_y} \cos \theta \qquad (6)$$

where

$$\theta = (\eta\tau + \phi),$$

and

x_o/x_y and ϕ are slowly varying functions of τ .

Applying the method of slowly varying parameters,(3) Equations (5) and (6) result in the expressions,

$$\left(\frac{\omega}{\omega_n}\right)^2 = C\left(\frac{x_o}{x_y}\right) \pm \frac{\sqrt{\left(\frac{F_o}{Q_y}\right)^2 \left[1 + \left|\frac{Q_o}{Q_y}\right|^{r-1}\right]^2 - \frac{16}{\pi^2}\left(\frac{r-1}{r+1}\right)^2 \left|\frac{Q_o}{Q_y}\right|^{2r}}}{\frac{Q_o}{Q_y}\left[1 + \left|\frac{Q_o}{Q_y}\right|^{r-1}\right]^2} \qquad (7)$$

where

$$C\left(\frac{x_o}{x_y}\right) = \frac{2}{\pi}\frac{x_y}{x_o}\int_0^{\pi} \frac{Q}{Q_y}\left(\frac{x_o}{x_y}\cos\theta\right)\cos\theta \, d\theta \qquad (8)$$

Q_o = the extreme value of the restoring force,

and

x_o = the displacement corresponding to Q_o .

Letting $\mu = x_o/x_y$, Equation (7) can be rewritten as,

$$(\frac{\omega}{\omega_n})^2 = C(\mu) \pm \sqrt{(\frac{F_o}{Q_y})^2 \frac{1}{\mu^2} - (\frac{r-1}{r+1}) [\frac{4}{\pi}(\mu - \frac{Q_o}{Q_y}) \frac{Q_o}{Q_y \mu^2}]^2} \qquad (9)$$

For the elasto-plastic case, it can be shown that Equations (7) and (8) reduce to

$$(\frac{\omega}{\omega_n})^2 = C\ (\mu) \pm \sqrt{(\frac{F_o}{Q_y})^2 \frac{1}{\mu^2} - [\frac{4}{\pi} \frac{(\mu - 1)}{\mu^2}]^2} \qquad (10)$$

$$C(\mu) = \frac{1}{\pi} \ [\cos^{-1} (1 - \frac{2}{\mu}) - 2\ (1 - \frac{2}{\mu}) \sqrt{\frac{\mu-1}{\mu^2}}\ ] \qquad (11)$$

Combining which result in the simple expression of,

$$(\frac{\omega}{\omega_n})^2 = \frac{1}{\pi} \ [\cos^{-1} (1 - \frac{2}{\mu}) - 2\ (1 - \frac{2}{\mu}) \ \frac{\mu-1}{\mu^2}\ ] \pm \sqrt{(\frac{F_o}{Q_y})^2 \frac{1}{\mu^2} - [\frac{4(\mu-1)}{\pi\mu^2}]^2} \qquad (12)$$

In order to check the accuracy of Equation (7), a numerical analysis of Equation (5) was performed on the digital computer. For given values of F_o/Q_y and ω/ω_n , values of x_o/x_y were found from Equation (7) and used as initial starting points in Equation (5). Then Equation (5) was solved numerically by using a fourth order Runge-Kutta method. The error for each trial point was calculated from $(x_i + x_f)^2 + \dot{x}_f^2$, where "i" and "f" stand for initial and final, respectively. With the help of a downhill climbing method an ineration procedure was established and the error minimized to the desired accuracy of less than 0.005. Figures 6 a-d and 7 show the results for various values of F_o/Q_y and exponent r .

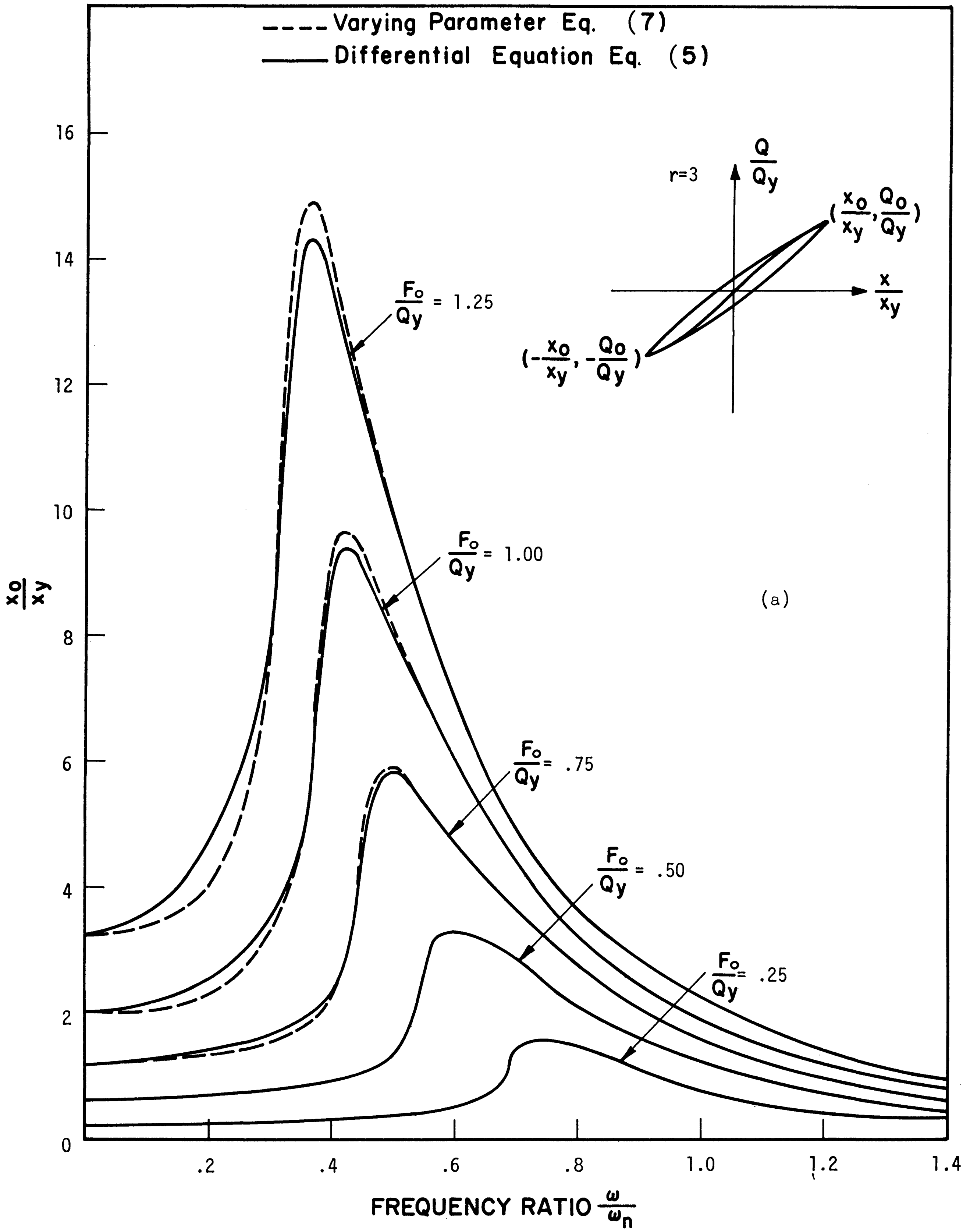

(a)

Figure 6. Steady-State Response Spectra for Ramberg-Osgood System.

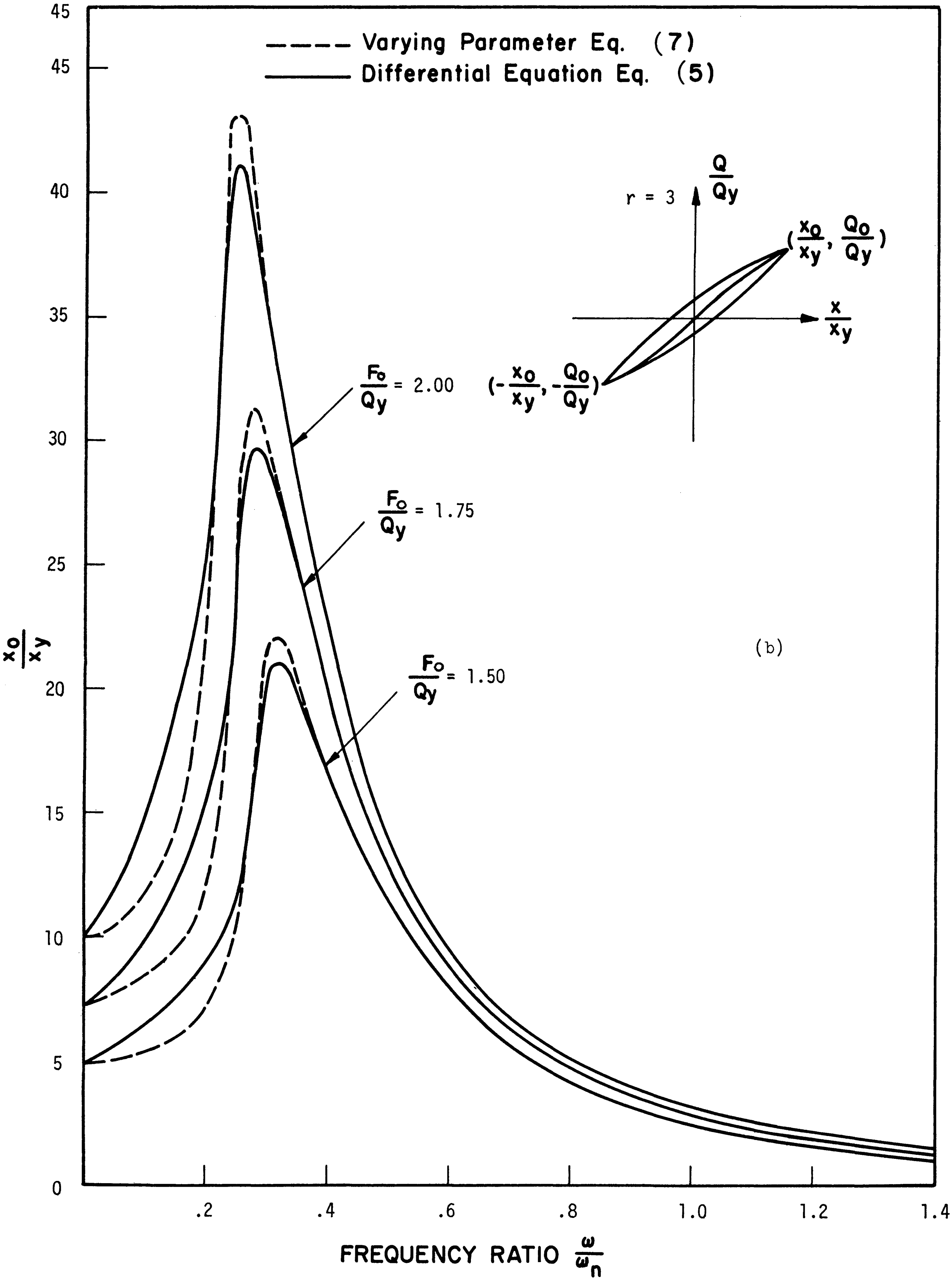

(b)

Figure 6. Continued.

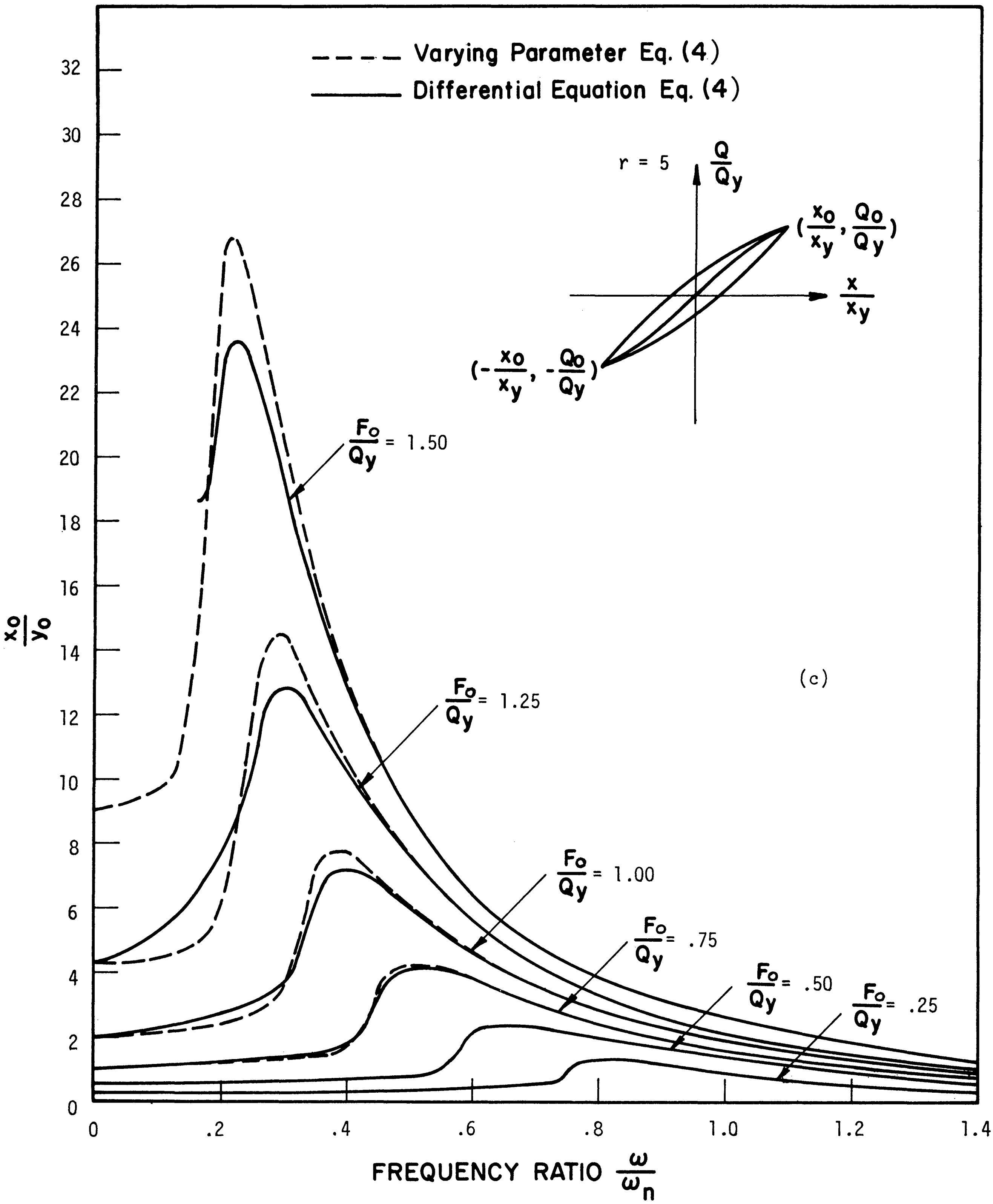

(c)

Figure 6. Continued.

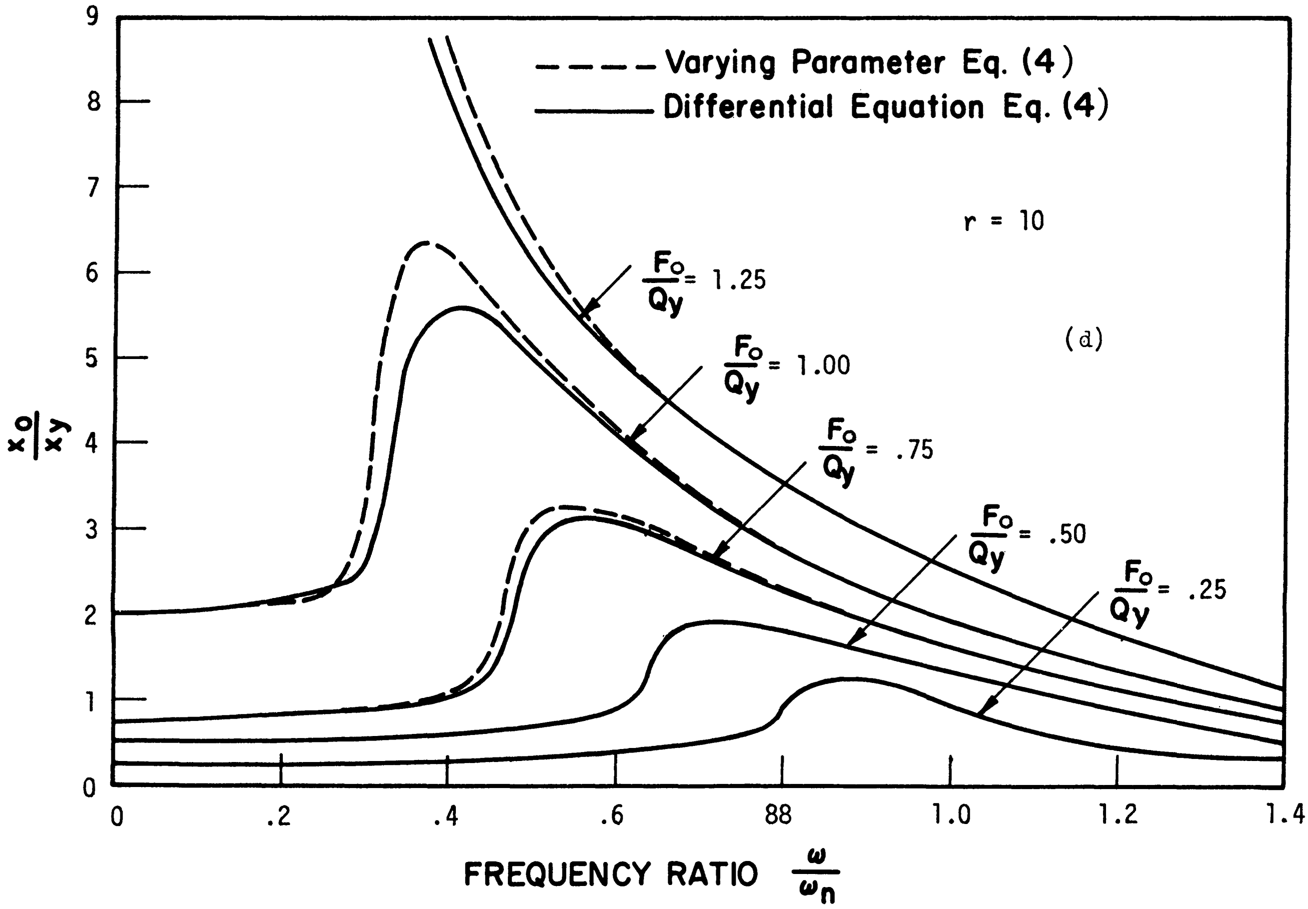

(d)

Figure 6. Continued.

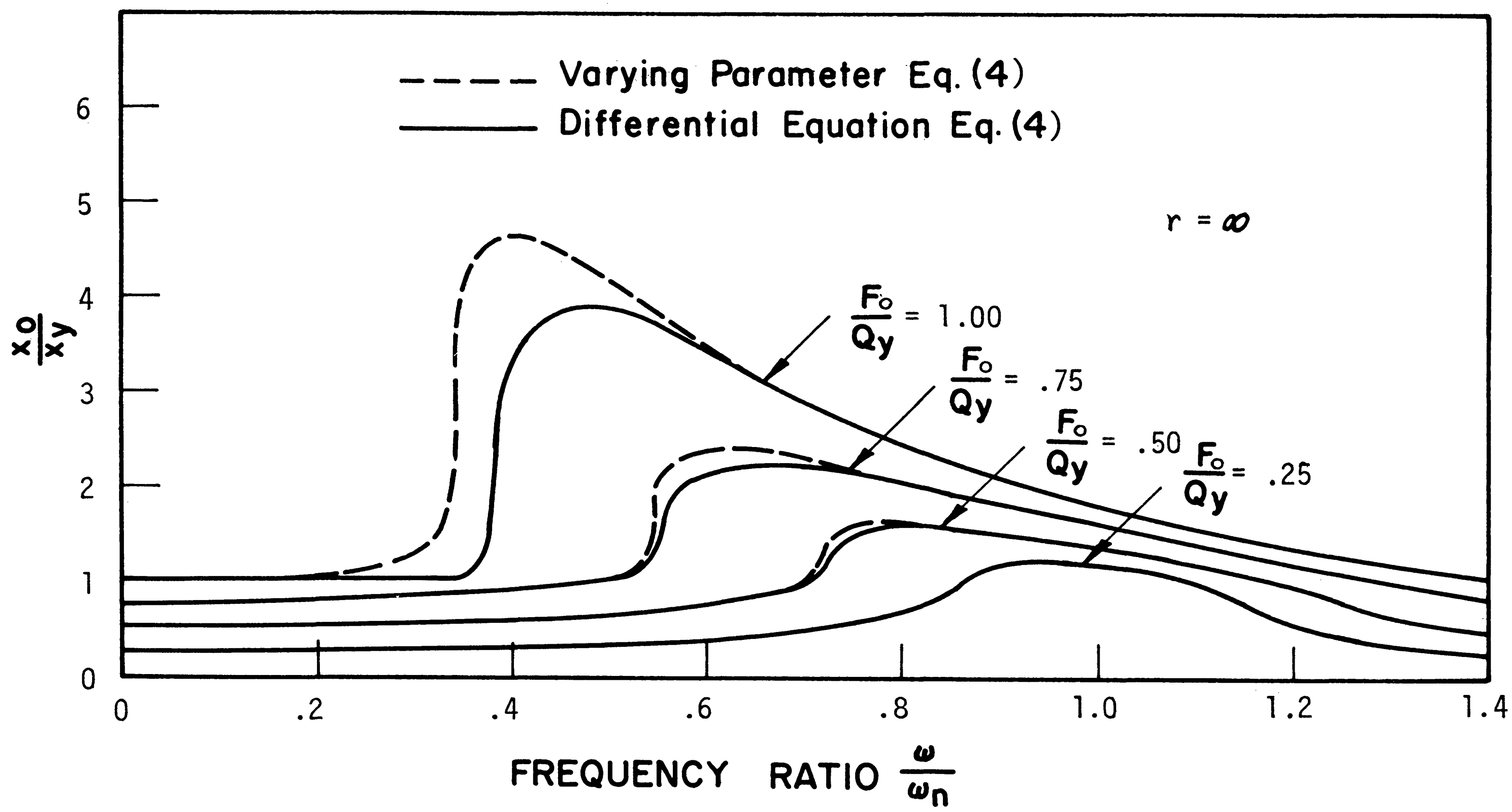

Figure 7. Steady-State Response Spectra for Elasto-Plastic System.

YIELD REVERSALS AND SIGNIFICANT RESPONSE PARAMETERS

Yield reversal is well defined in the elasto-plastic system. However, the Ramberg-Osgood system has no single defintion for it. A sliding $2x_y$ criterion is used in this report for yield reversal i.e. when the absolute difference between displacements x_i (current extreme point obtained by loading in one direction) and x_{i+1} (obtained by loading in opposite direction) is greater than twice the value of x_y , yield reversal is reached. Expressed in equation form this becomes $|x_i - x_{i+1}| > |2x_y|$. A detailed description of this criterion is found in Figure 8.

The effect of yield level upon the number of yield reversals, for various values of Ramberg-Osgood exponent only, is shown in Figure 9 for El Centro 1940 NS.

Two response parameters, namely, the ductility and the energy ratios, provide a meaningful characterization of the response of an inelastic system to earthquake. The ductility ratio μ is defined as the ratio of the maximum displacement to the yield displacement, $\mu = x_{max}/x_y$. The energy ratio ϵ is defined as the ratio of the maximum strain energy input per unit mass E_s , to the recoverable strain energy per unit mass at yield, $\epsilon = 2(E_s)_{max}/q_y x_y$.

The excursion ratio ϵ_x for the Ramberg-Osgood function is defined as the sum of all deformation in the yield regions produced during the earthquake, to the yield deformation x_y (see Figure 8). The total energy dissipated by hysteresis in a Ramberg-Osgood system is related to the excursion ratio. However, unlike the elasto-plastic case there is no simple way of converting hysteresis energy to excursion ratio.

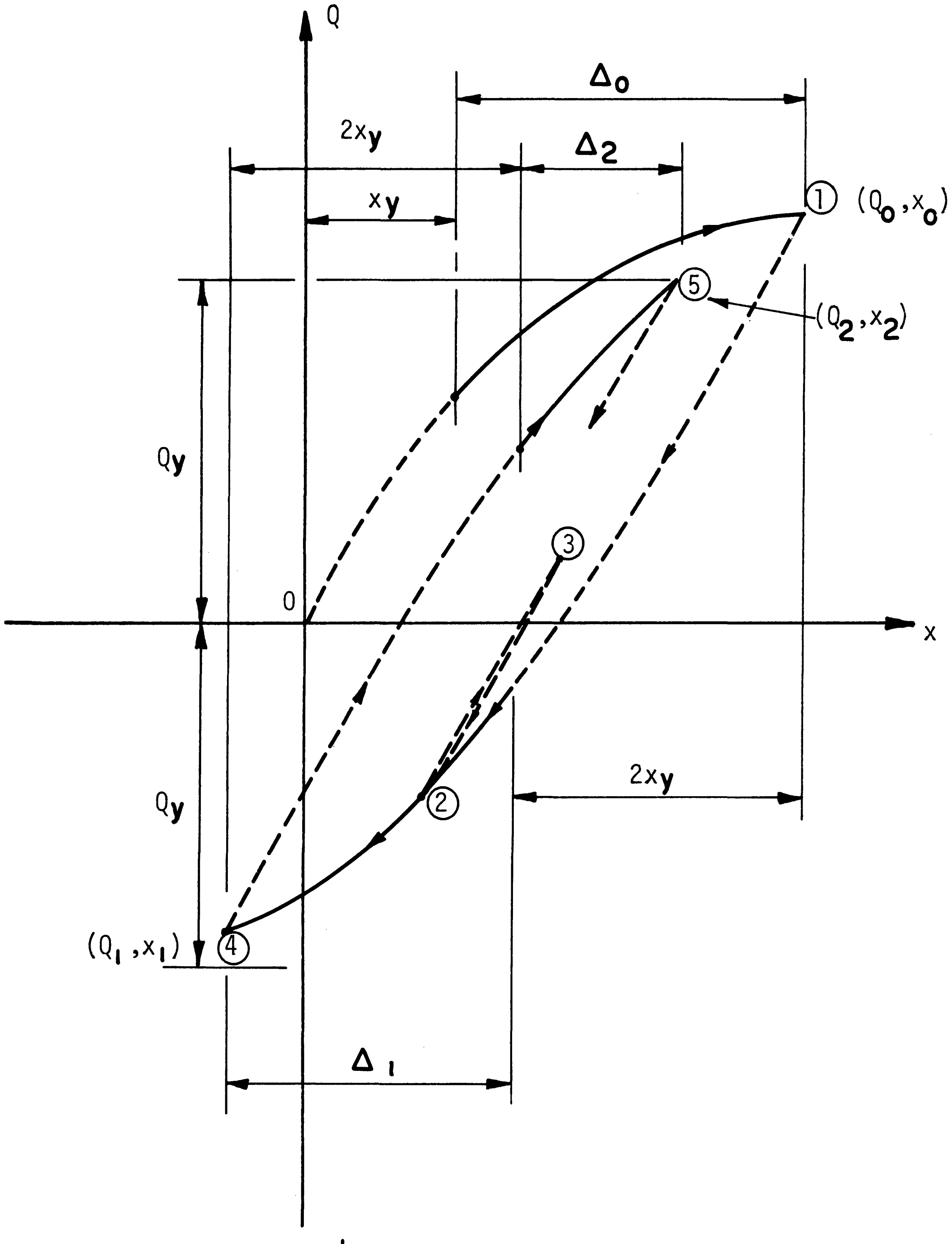

$$\epsilon_x = \frac{1}{x_y}(\Delta_0 + \Delta_1 + \Delta_2)$$

Figure 8. Yield Reversal Criterion and Excursion Ratio for Ramberg-Osgood Systems.

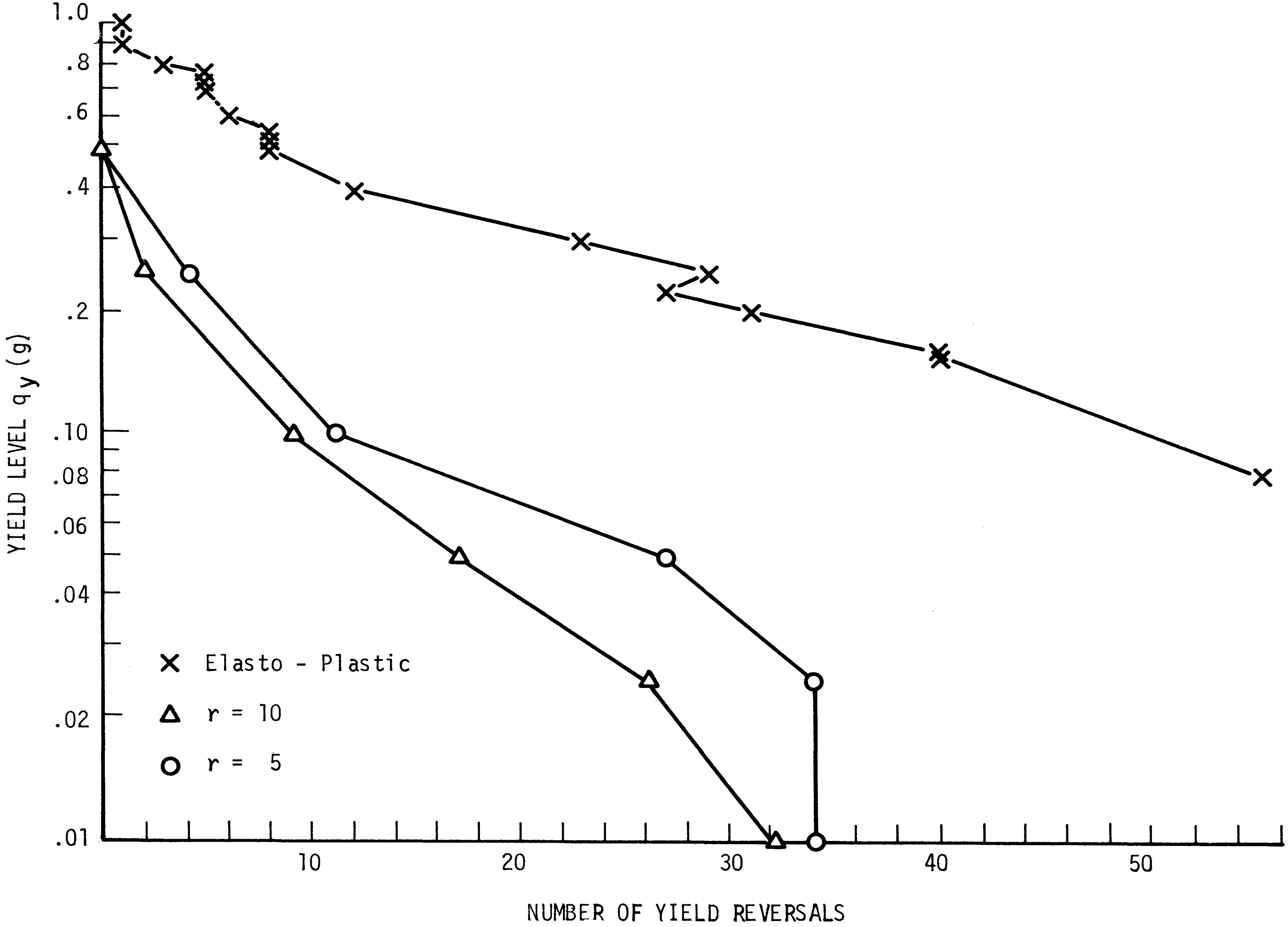

Figure 9. Yield Level q_y vs. Number of Yield Reversals, El Centro, May 18, 1940, N-S Component.

If all yielding occurred in the same direction, the relation between the energy and ductility ratios for the Ramberg-Osgood system, can be given as

$$\epsilon = \frac{Q_o/Q_y}{r + 1} \; [2r\,\mu - (r-1)\,\frac{Q_o}{Q_y}\,] \qquad (13)$$

in any case

$$\epsilon \geq \frac{Q_o/Q_y}{r + 1} \; [2r\,\mu - (r-1)\,\frac{Q_o}{Q_y}\,] \qquad (14)$$

When $r = \infty$, Equation (14) results in the elasto-plastic case, i.e. $\epsilon \geq 2\mu - 1$.

The energy ratio ϵ has been proposed as a more critical parameter in inelastic earthquake design than the ductility ratio μ , because it is felt that the energy ratio along with the number of times the system reverses during the earthquake, will help provide a better indication of how a structure would perform in a strong-motion earthquake.

RESPONSE SPECTRUM CONCEPTS

The maximum of the absolute value of x , x and $(x + y)$ can be evaluated for various parameters from Equation (2), and plotted against the period as displacement, velocity and acceleration spectra respectively.

The maximum spring force Q_m can be expressed as

$$Q_m = C_s W \quad . \tag{15}$$

where the lateral load coefficient C_s corresponds to $|x + y|_{max}/g$, and W equals the weight (mg) of the system.

(a) For linear systems these spectra have the relation

$$\omega_n |x|_{max} \approx |x|_{max} \approx \frac{|x+y|_{max}}{\omega_n} \tag{16}$$

This expression is exact for undamped linear systems and is a good approximation when damping is small.

If the velocity spectrum is plotted on a log-log scale, because of Equation (16) relationship, logarithmic diagonal scales can be constructed, (for displacement sloping up to the right, and for acceleration sloping up to the left), and values of all response spectra ($|x|_{max}$, $|\dot{x}|_{max}$, and $|\ddot{x} + \ddot{y}|_{max}$) read directly from the same plot. See solid line in Figure 12a.

(b) In elasto-plastic systems, since the spring force is equal to Q_y when displacements are in excess of x_y , the absolute maximum displacement and the absolute maximum acceleration are related as follows,

$$\omega_n \quad \frac{|x|_{max}}{\mu} \approx \frac{|\ddot{x} + \ddot{y}|_{max}}{\omega_n} \qquad (17)$$

Again this relation is exact when damping is zero; otherwise it is approximate because it does not take the damping force into account.

A plot of $\omega_n \; |x|_{max}/\mu$ against period T on a log-log scale, for specified ductility (or energy) and damping ratios, results in a pseudo velocity response spectra.(9, 10) (Pseudo in the sense that $\omega_n \; |x|_{max}/\mu$ is not equal to the absolute maximum velocity $|\dot{x}|_{max}$, for there exists a discrepancy between the two and this discrepancy increases with increasing values of μ.)

From Equation (17) and the pseudo-velocity concept, diagonal log scales can be constructed on the chart as was done in the elastic case, and the maximum displacement $|x|_{max}/\mu$, and the maximum acceleration $|\ddot{x} + \ddot{y}|_{max}$ read from the diagonal scales directly. A typical example is shown in Figure 12a.

(c) The relation between $\omega_n \; |x|_{max}/\mu$ and $|\ddot{x} + \ddot{y}|_{max}/\omega_n$ established in the elasto-plastic system is generally not valid for Ramberg-Osgood systems. Thus it is inadvisable to make a four way log-log plot.(9)

The displacement and the acceleration spectra for Ramberg-Osgood systems are plotted separately on three way log-log plots as seen in Figures 10a and 10c.

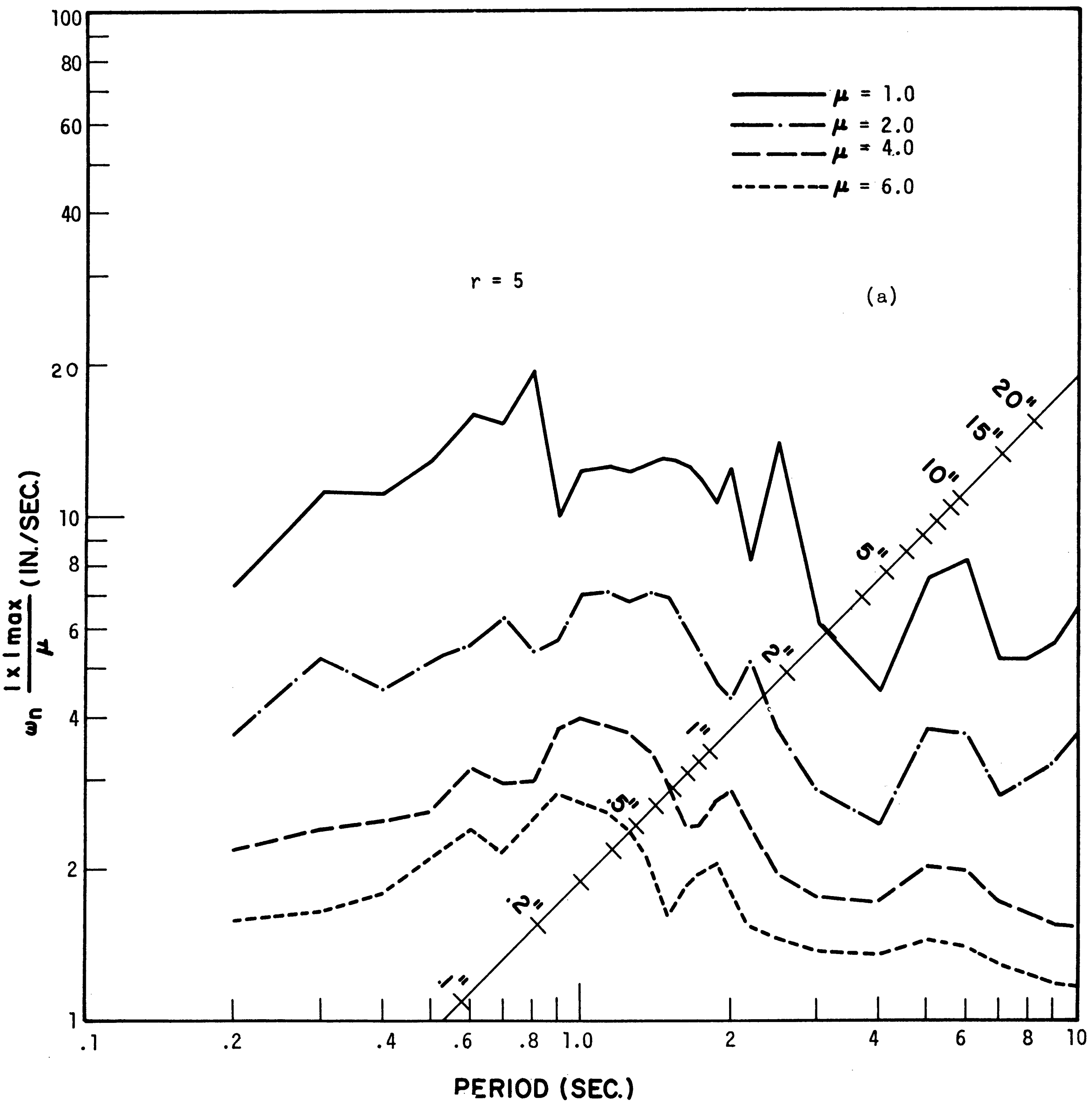

(a)

Figure 10. Displacement Spectra for Ramberg-Osgood System, Taft, July 21, 1952, S21°W. Constant ductility ratio "μ".

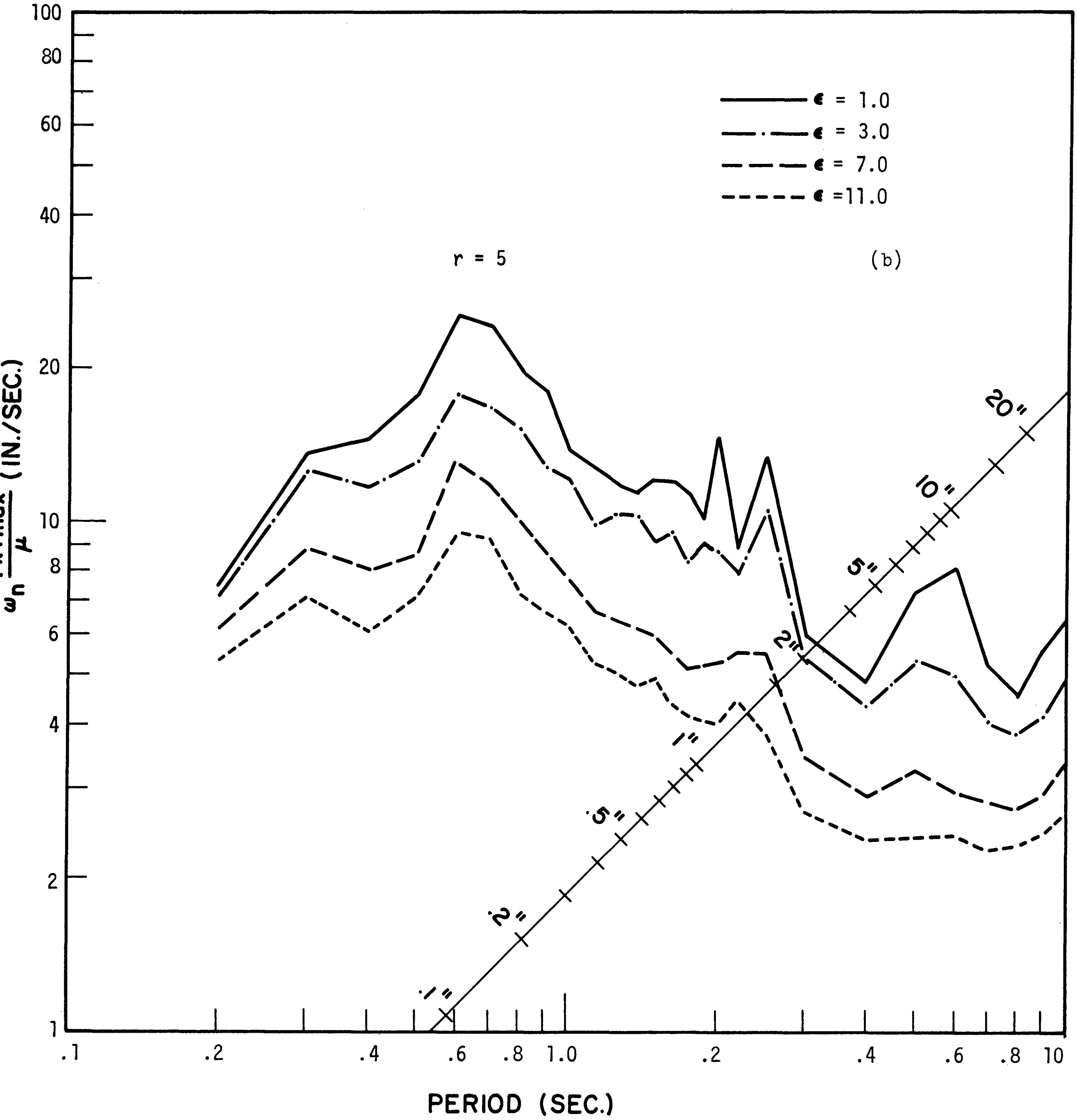

(b)

Figure 10. Continued.

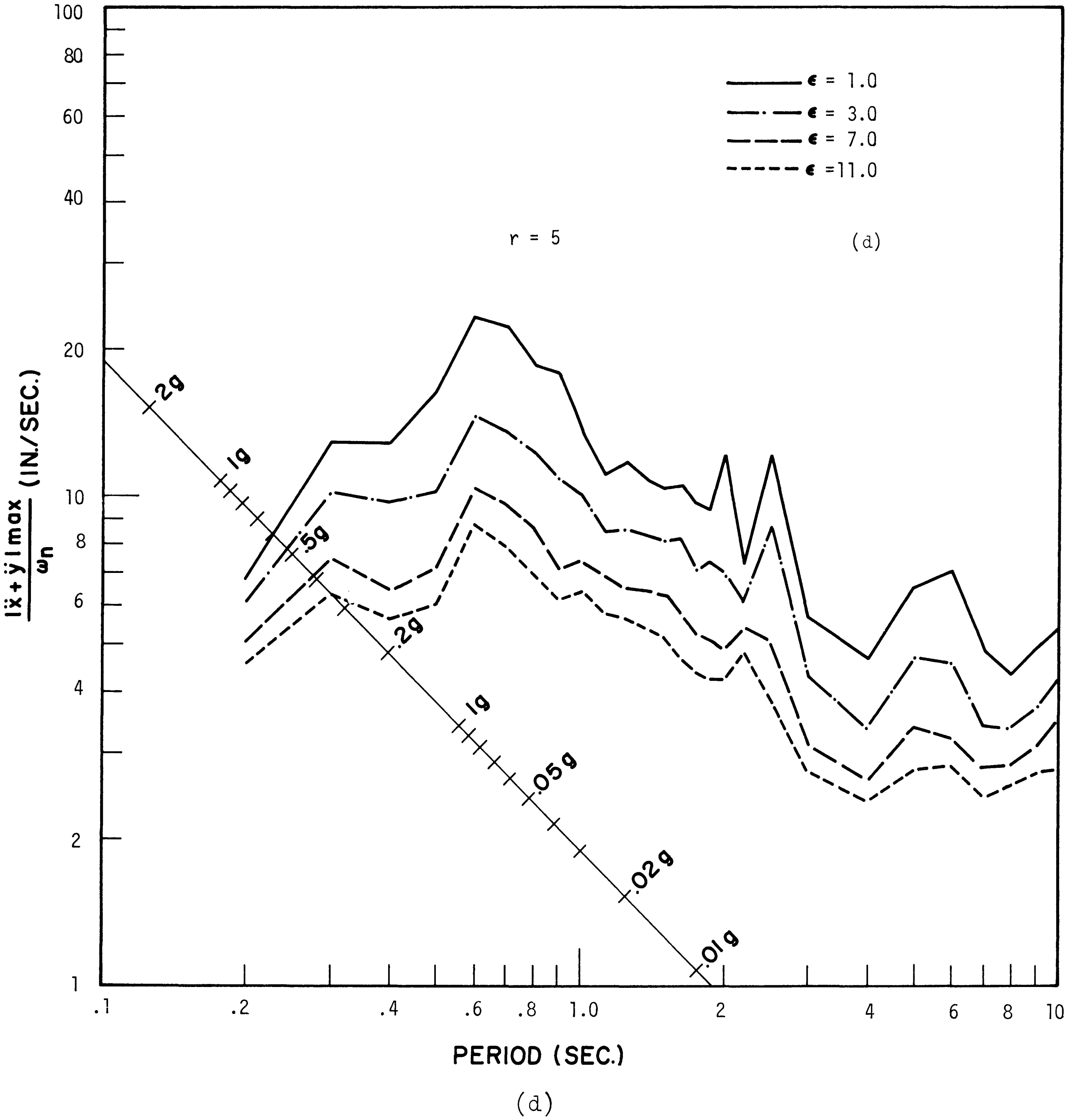

(d)

Figure 10. Continued.

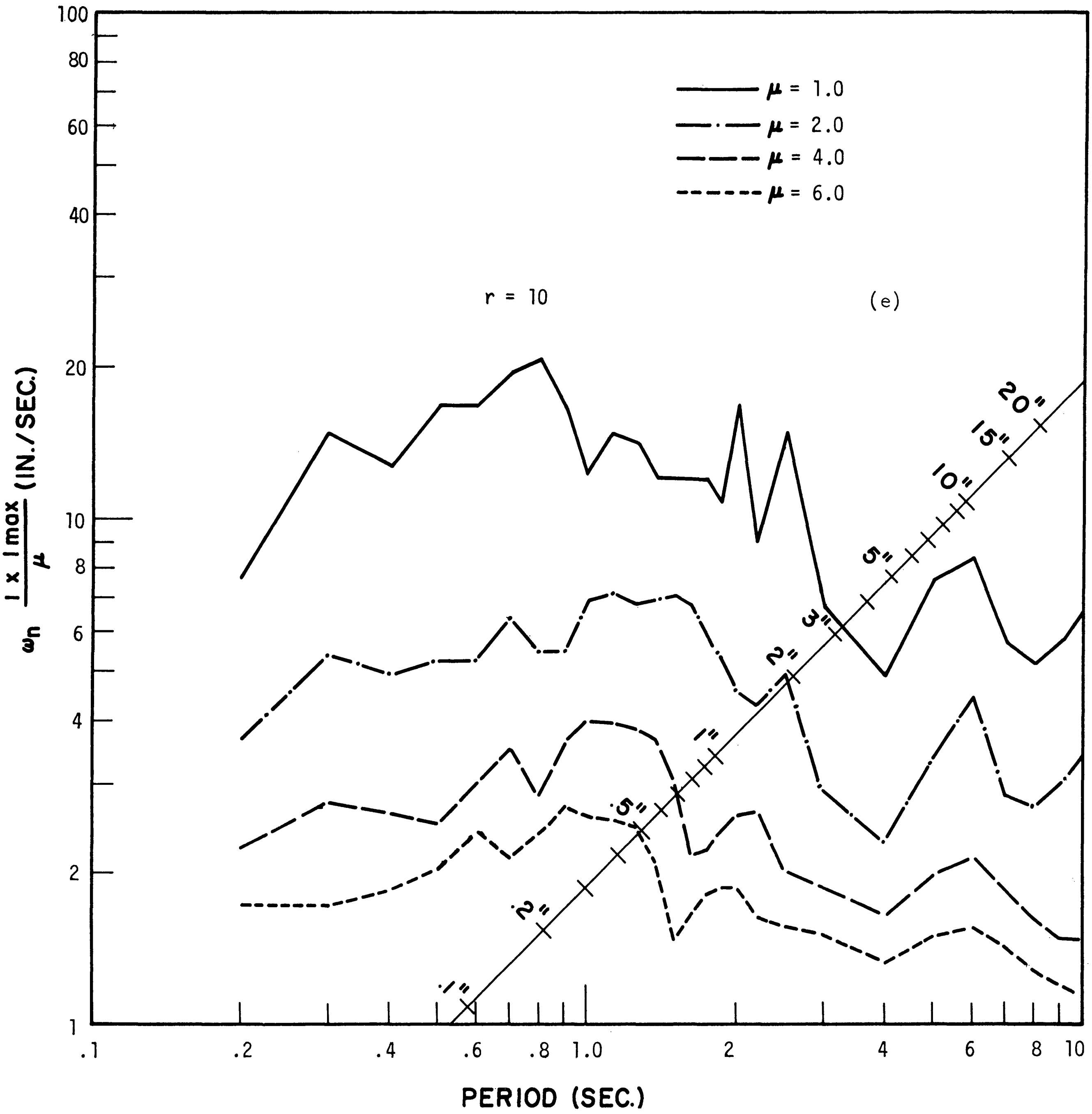

(e)

Figure 10. Continued.

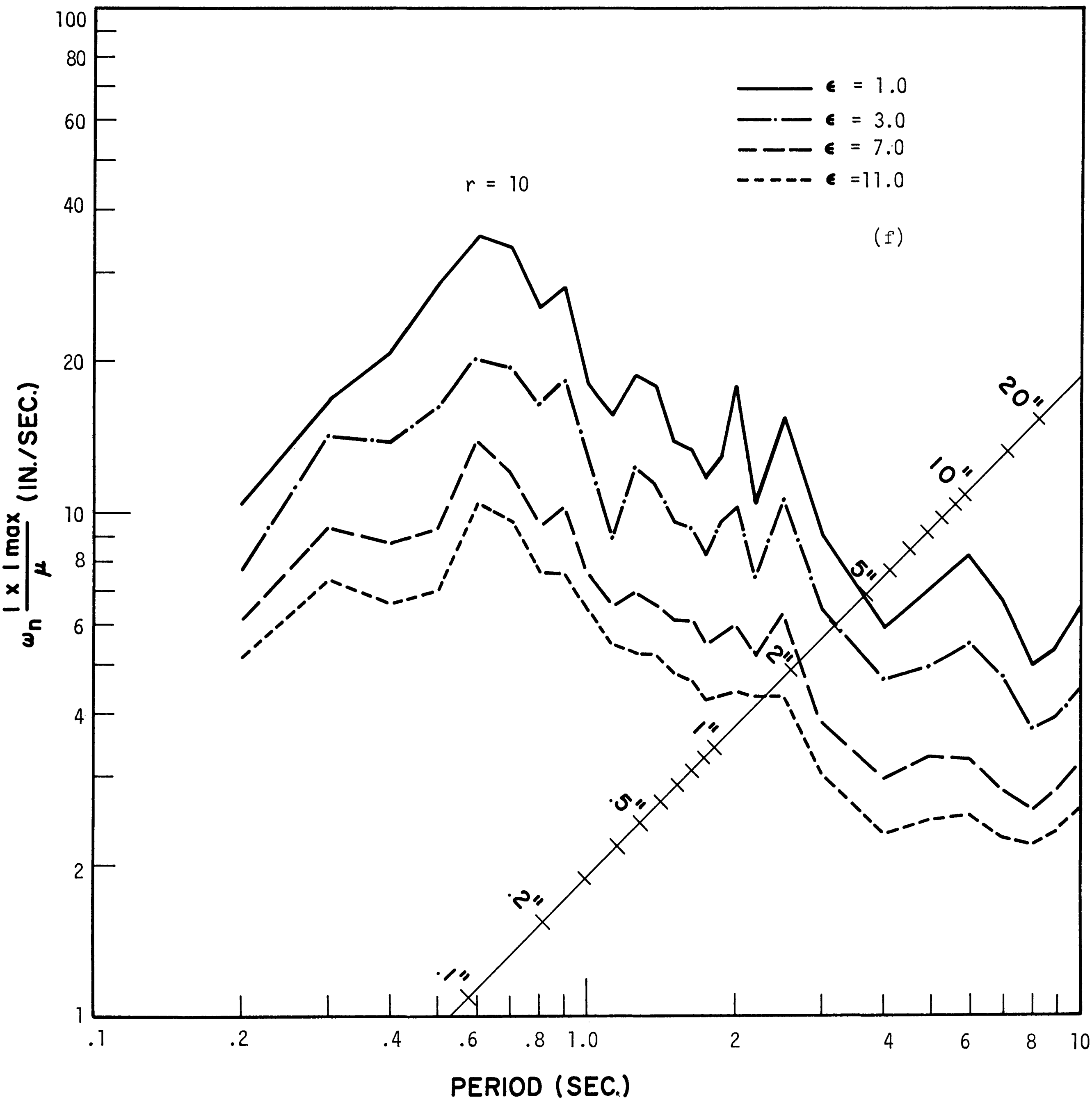

(f)

Figure 10. Continued.

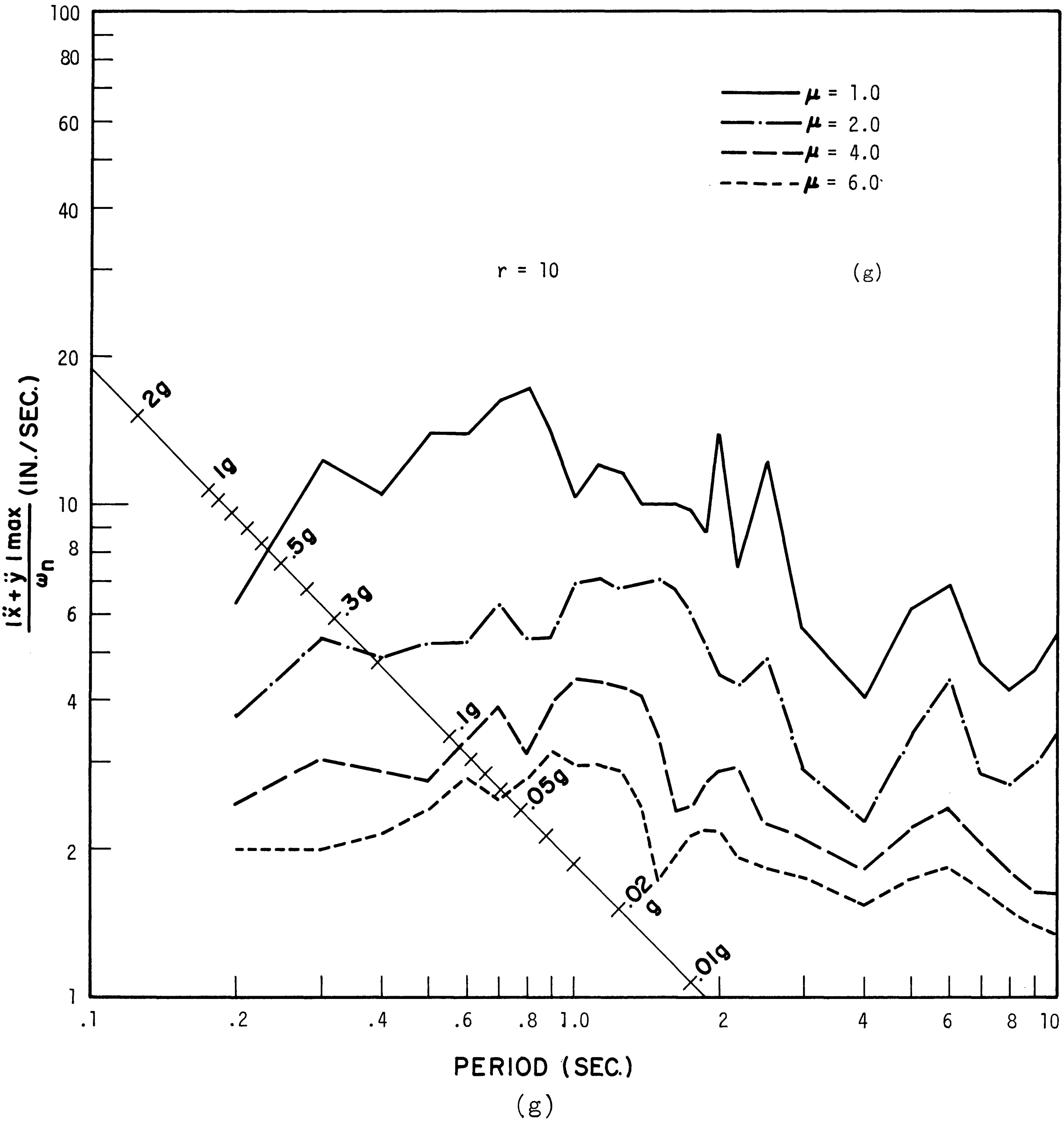

Figure 10. Continued.

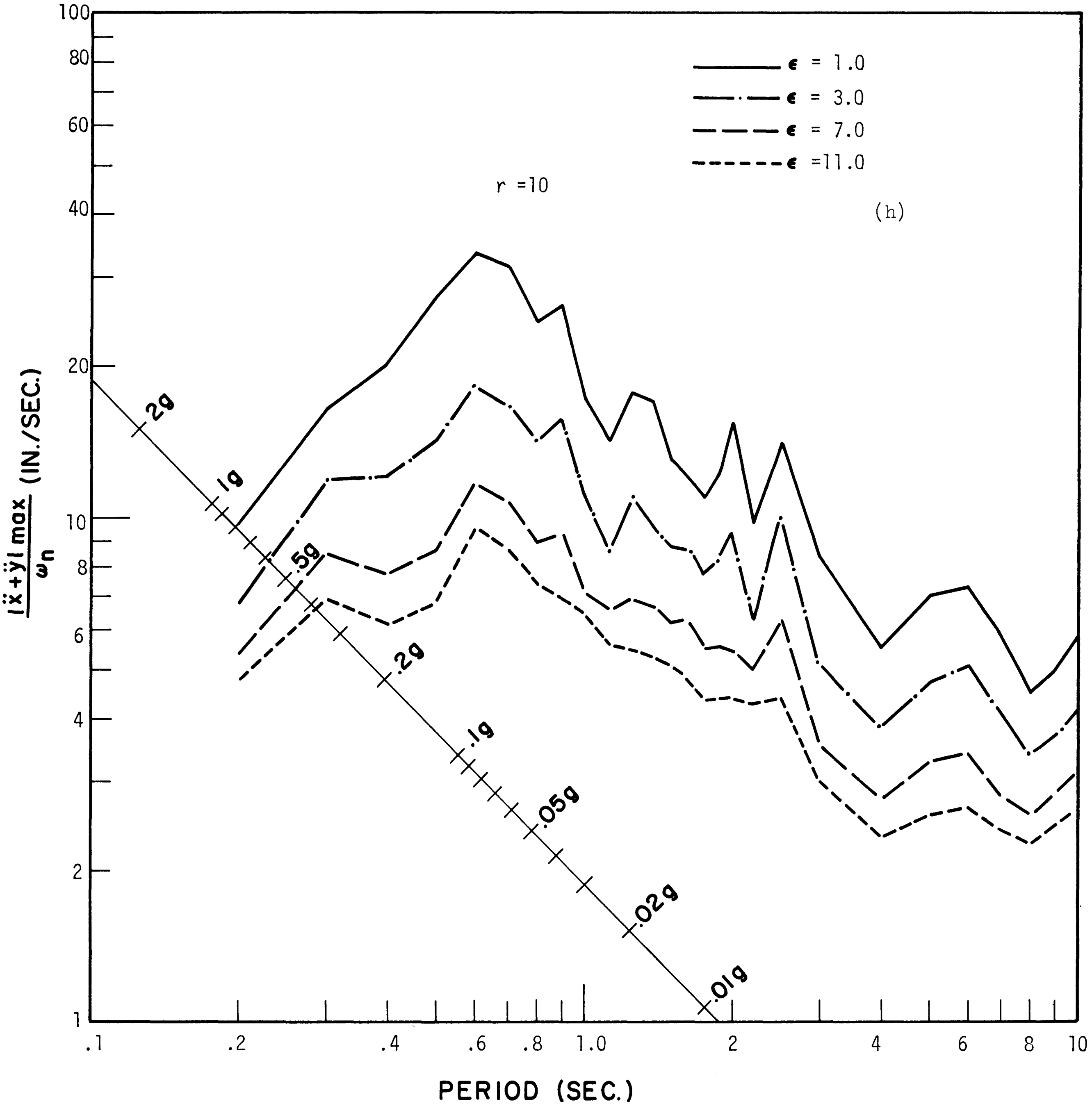

(h)

Figure 10. Continued.

RAMBERG-OSGOOD RESPONSE SPECTRA FOR TWO STRONG-MOTION EARTHQUAKES

Equation (4) was evaluated numerically for various values of q_y , x_y and r . A fourth-order Runge-Kutta procedure was used for this purpose on the 7090 digital computer at the University of Michigan. The method used to obtain a response with a desired value of ductility on energy ratio was as follows:

The responses for a number of systems with arbitrarily assigned yield levels were first computed. Then a linear interpolation method was adopted to interpolate between the obtained responses in order to determine the approximate yield levels which would give the desired results. These yield levels were used as input data and the corresponding responses calculated. This procedure was repeated until the desired responses were obtained.

The values of r were chosen to be 5 and 10. To compare these parameters, ductility ratios of 1.0, 2.0, 4.0, and 6.0 were considered, and the corresponding spectra were computed directly by the digital computer. The spectra for energy ratios of 1.0, 3.0, 7.0 and 11.0 were obtained by interpolating the computed data above.

The input function $\ddot{y}(t)$ consisted of punched card accelerograms[11] of the following two strong-motion earthquakes:

Taft, California	S21W	July 21, 1952
Olympia, Washington	S86W	April 29, 1965

The response spectrum curves presented, Figures 10 and 11, were constructed throughout on the basis of the maximum displacement or the maximum acceleration which occurred within the 30 second duration of the earthquake.

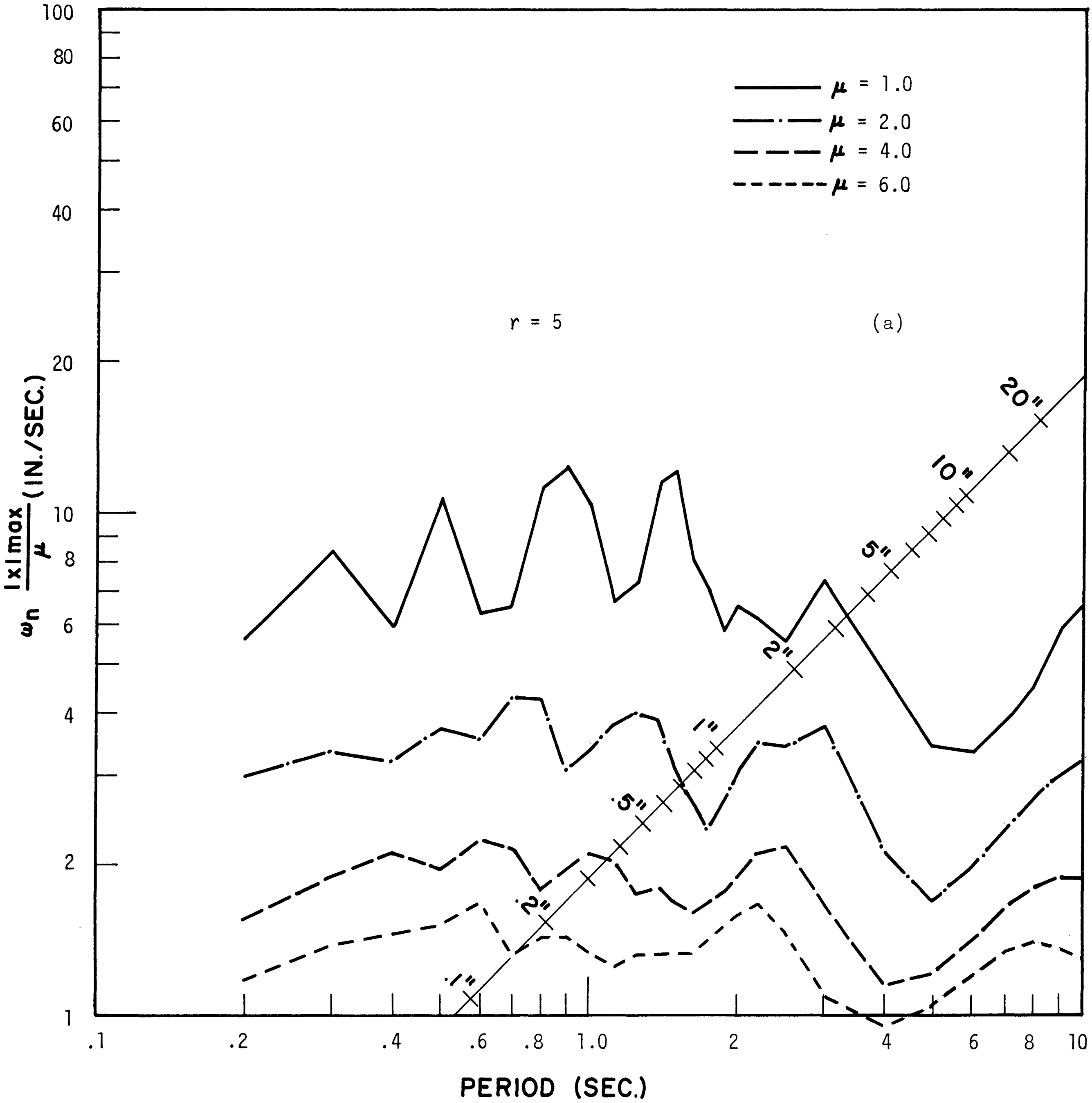

(a)

Figure 11. Displacement Spectra for Ramberg-Osgood System, Olympia, April 29, 1965, S86°W. Constant ductility ratio "μ".

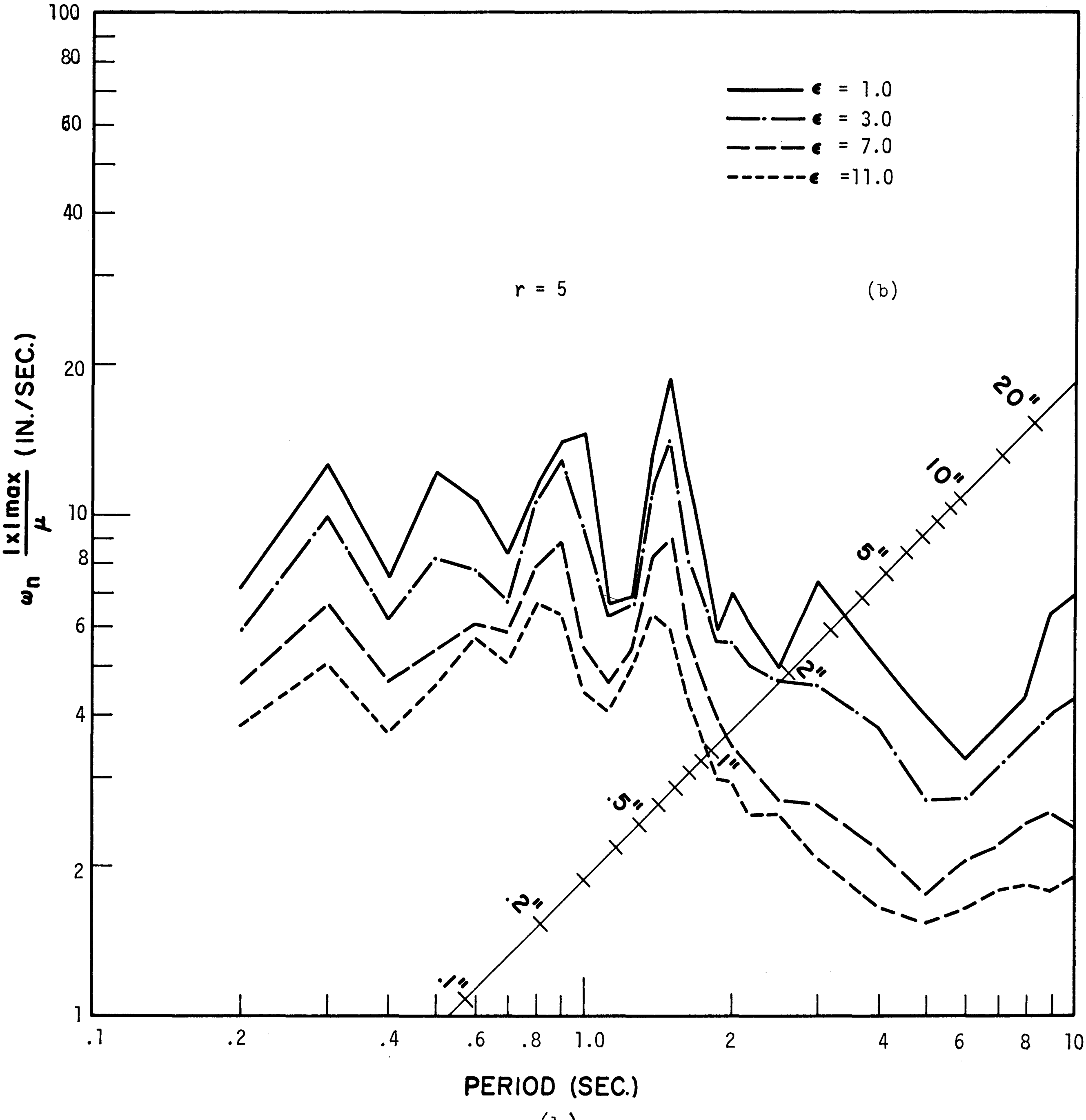

(b)

Figure 11. Continued.

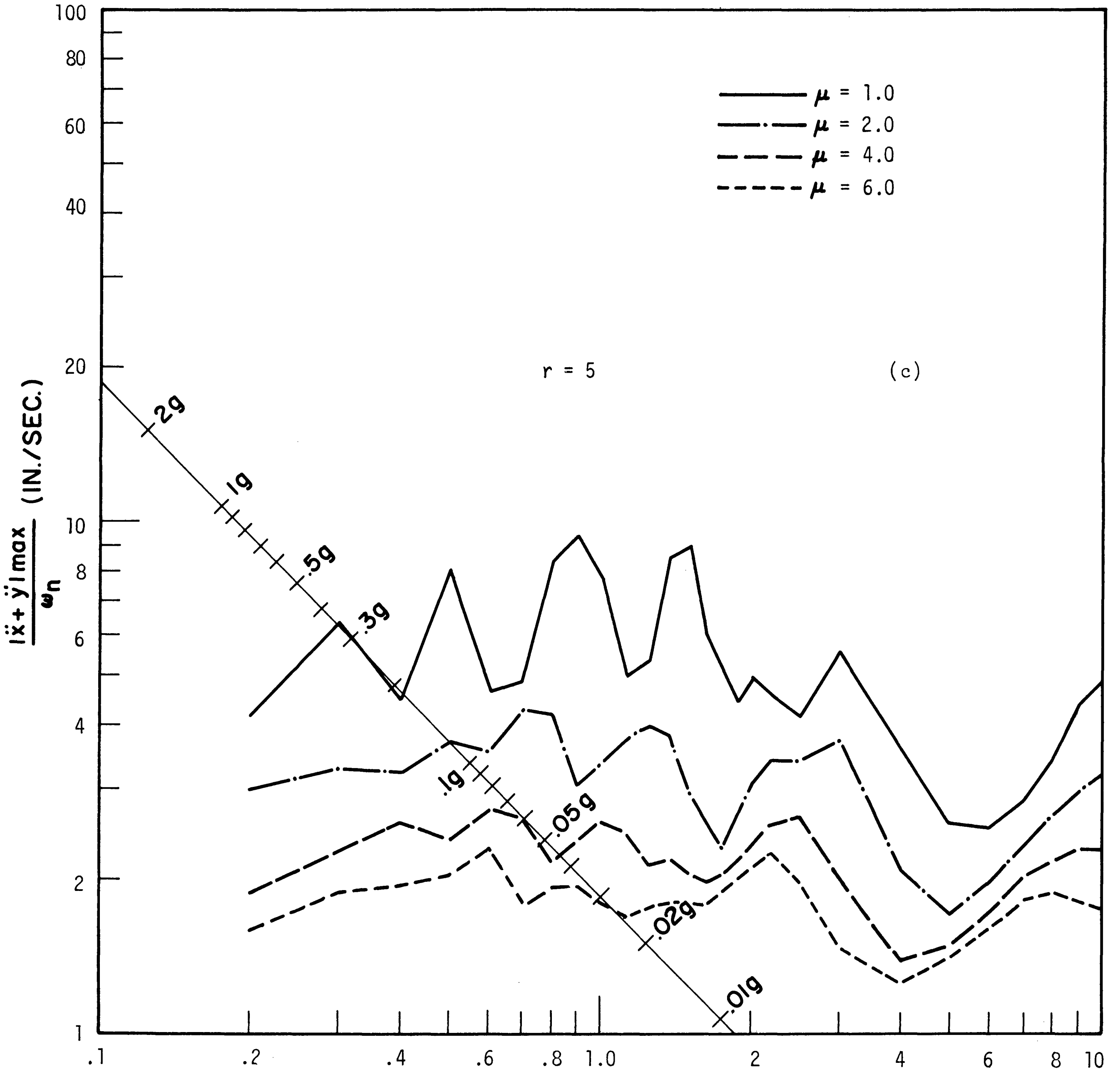

(c)

Figure 11. Continued.

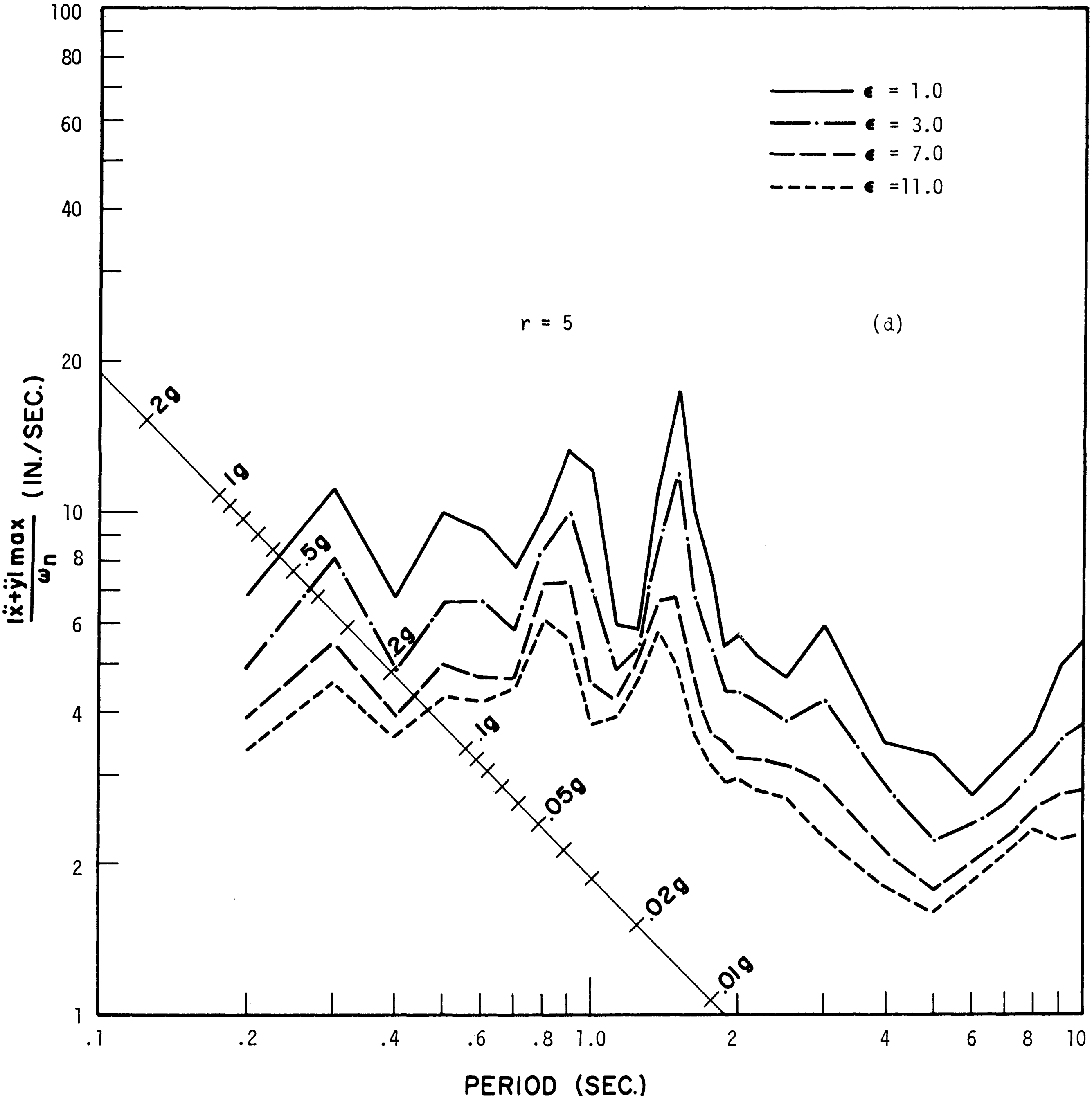

(d)

Figure 11. Continued.

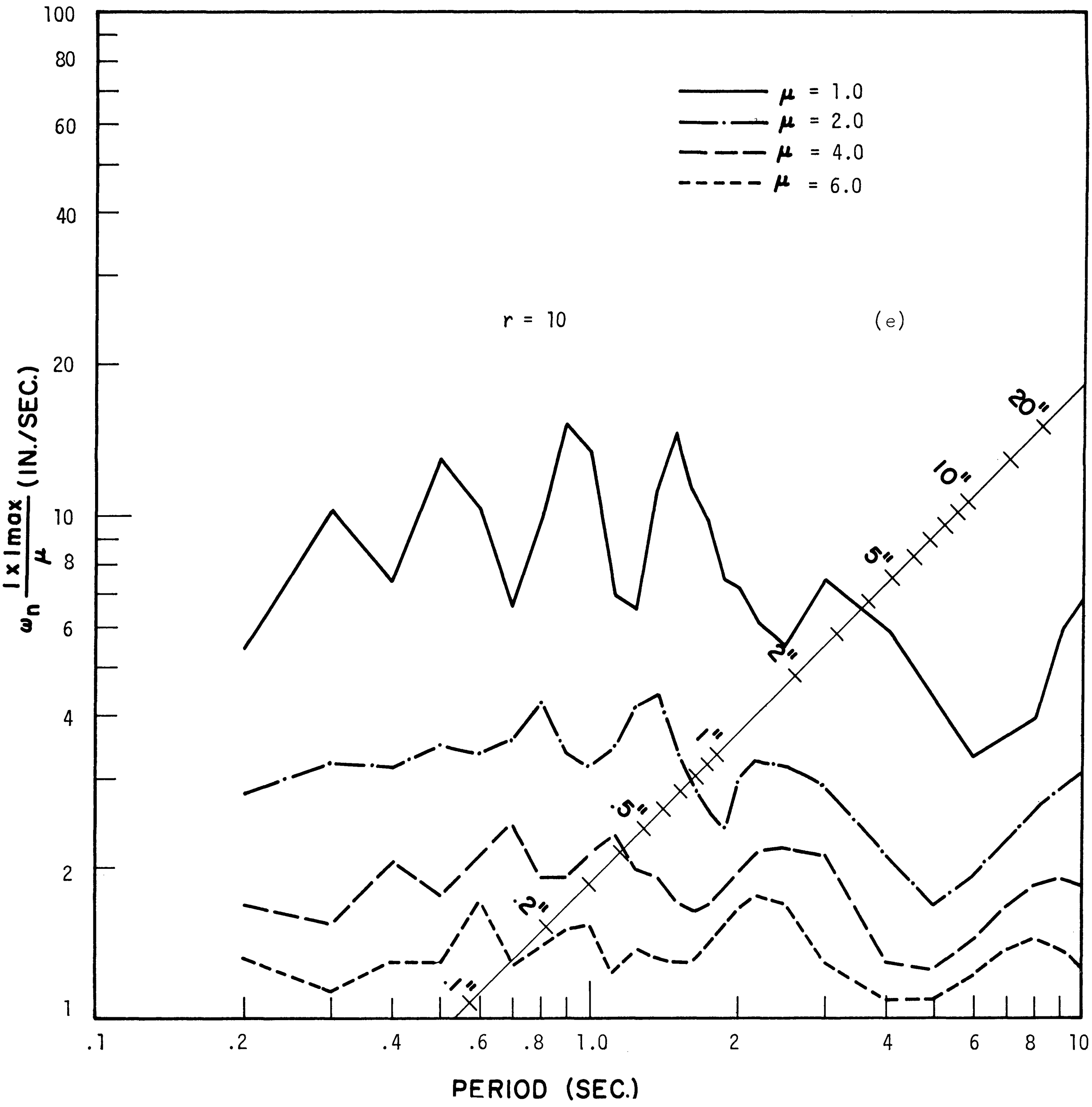

(e)

Figure 11. Continued.

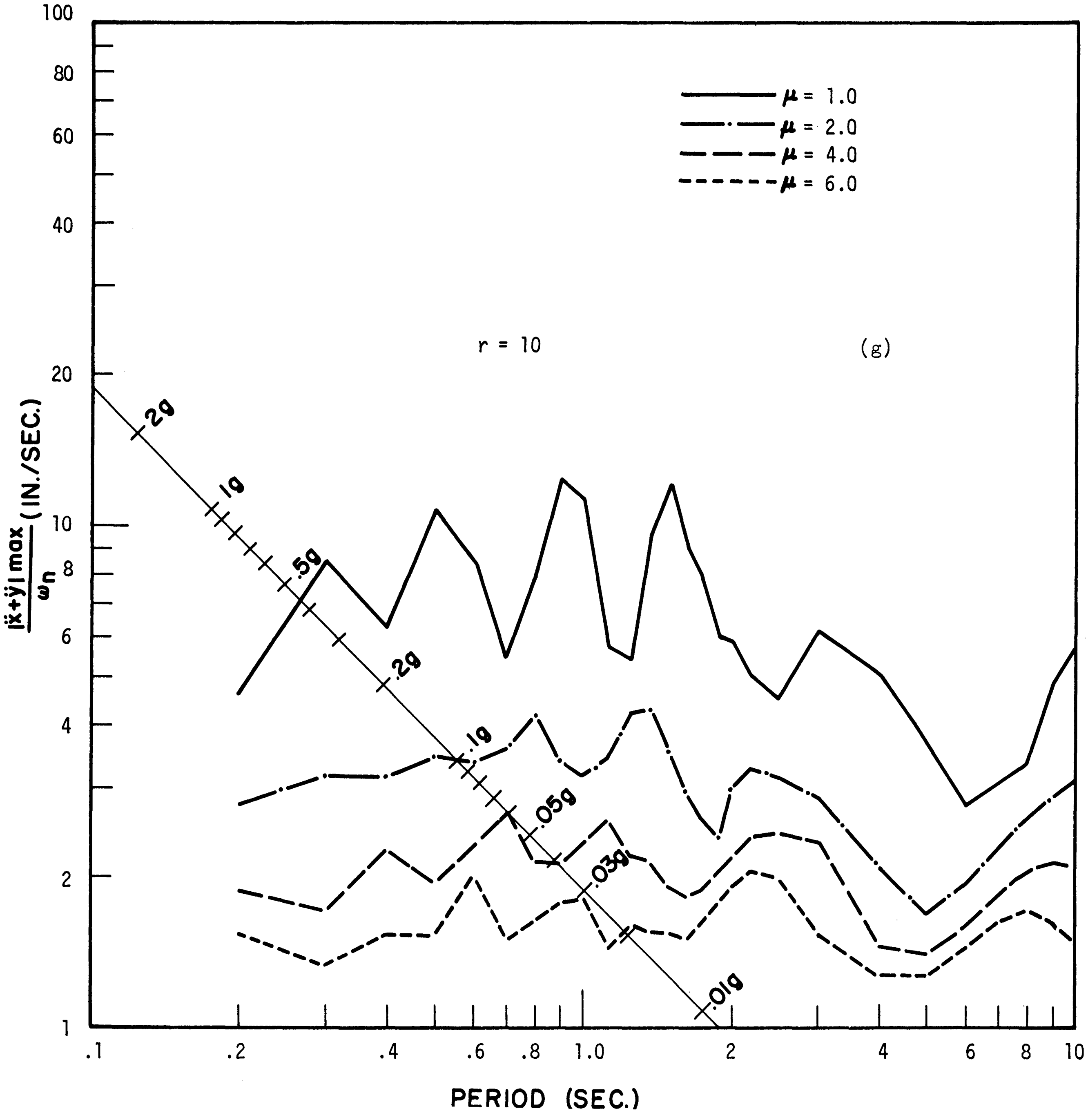

(g)

Figure 11. Continued.

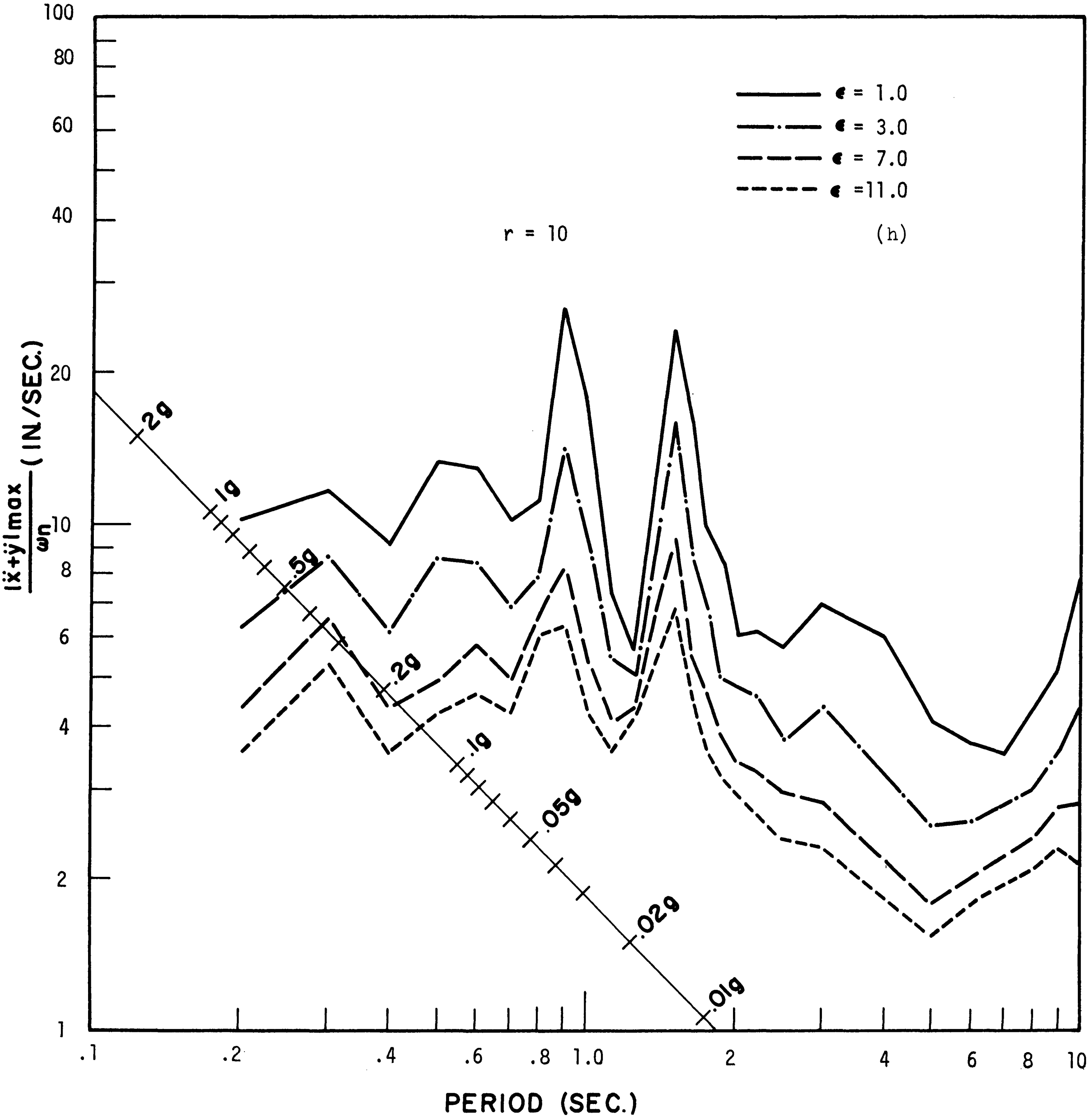

(h)

Figure 11. Continued.

Response spectra for $r = \infty$, i.e. the elasto-plastic case, are also included in this report for the above accelerograms as well as for El Centro 1940 S, and are shown plotted in Figures 12 through 14. For ductility ratio $\mu = 1$, the elasto-plastic system reduces to the elastic system. Hence the solid lines in these figures represent the response spectra of linear systems.

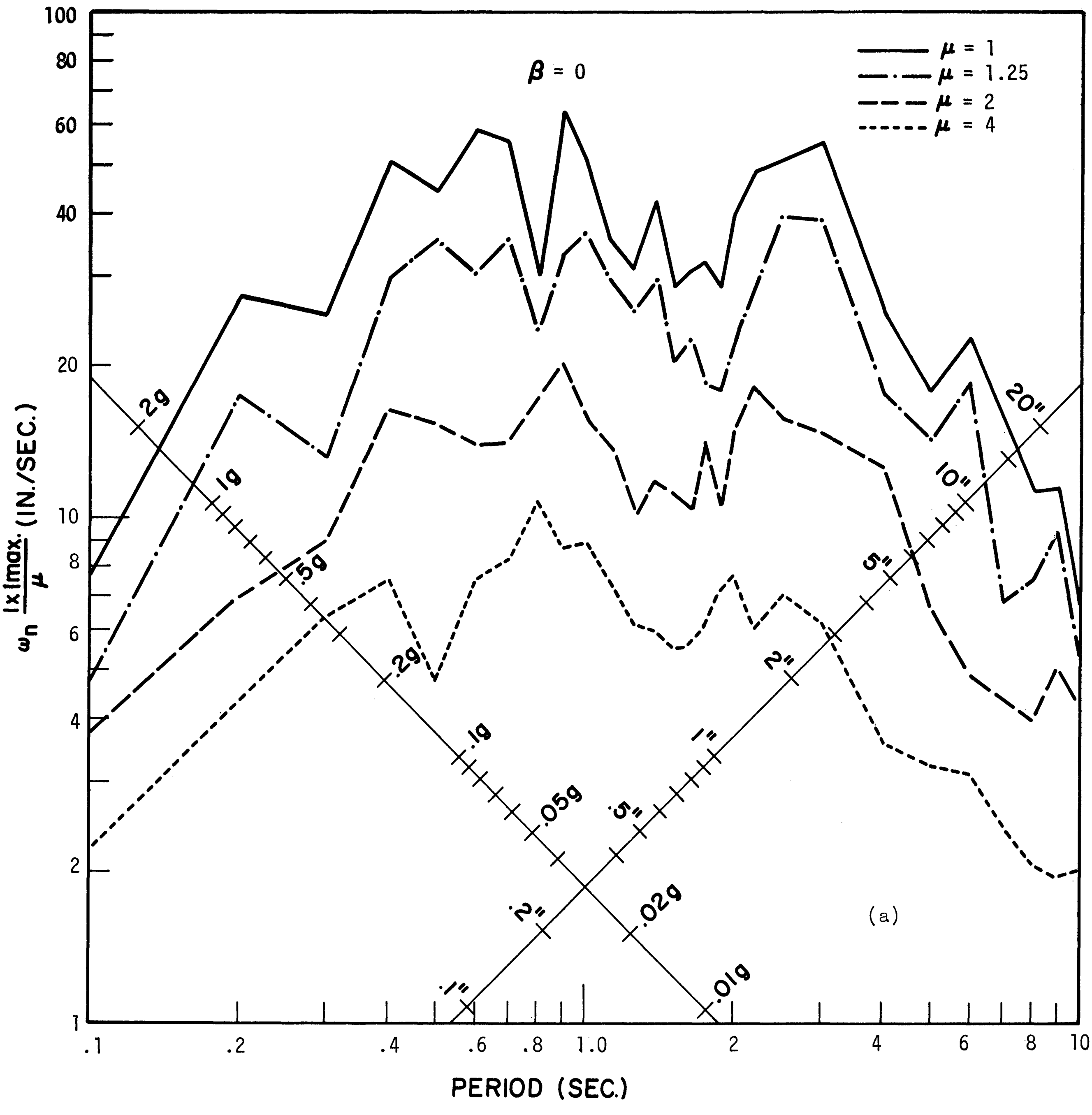

(a)

Figure 12. Response Spectra for the Elasto-Plastic System, El Centro, May 18, 1940, S. Constant ductility ratio "μ".

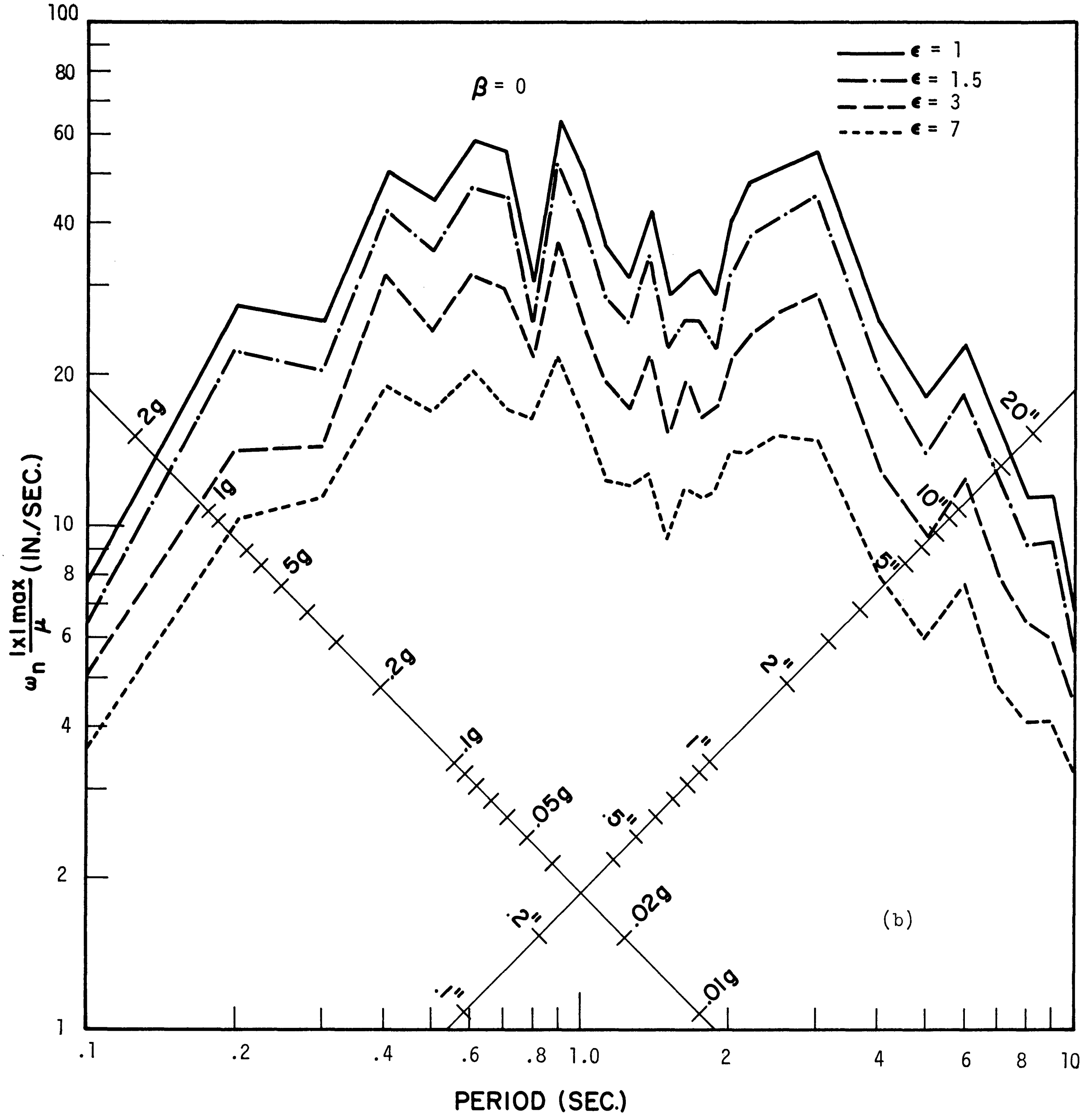

(b)

Figure 12. Continued.

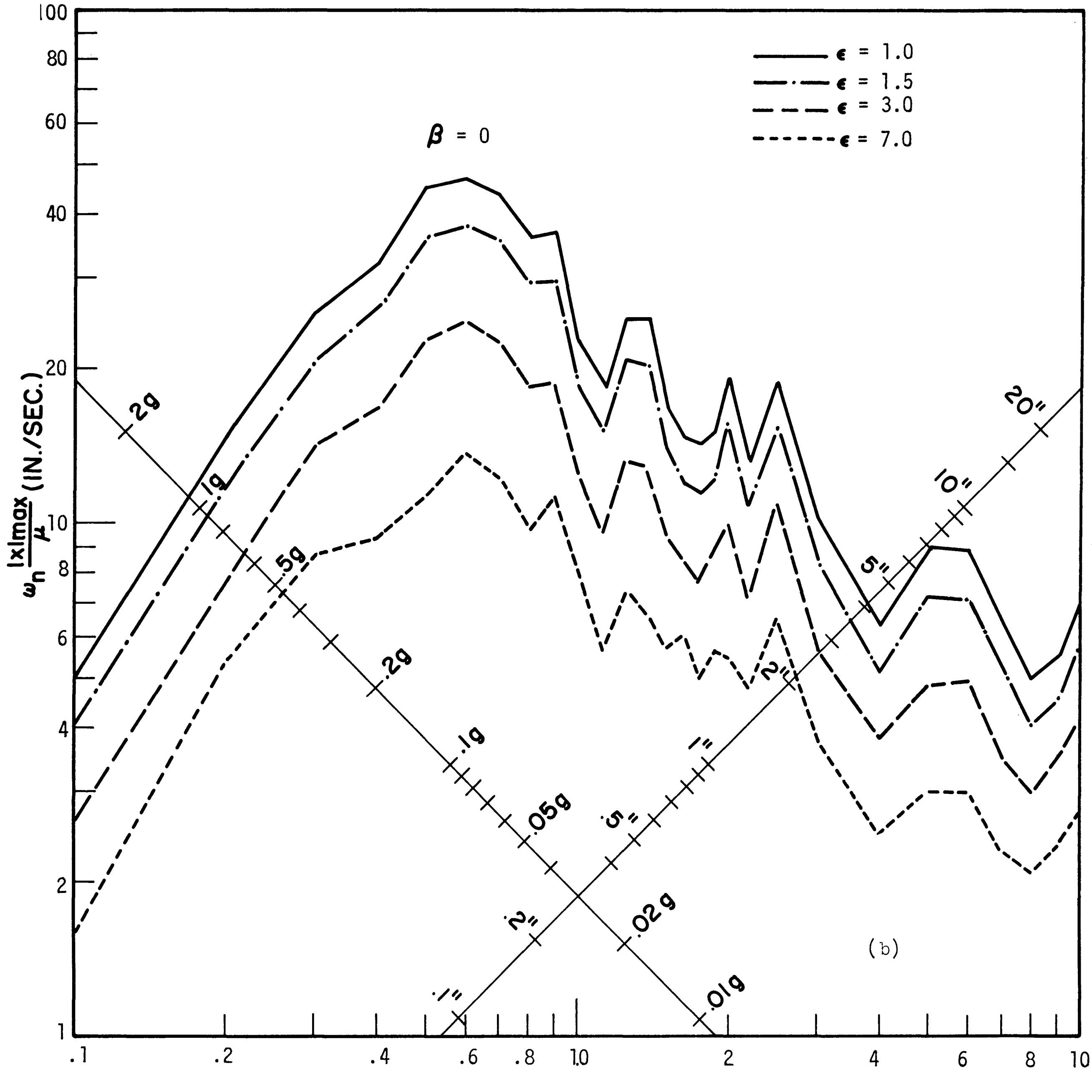

(b)

Figure 13. Continued.

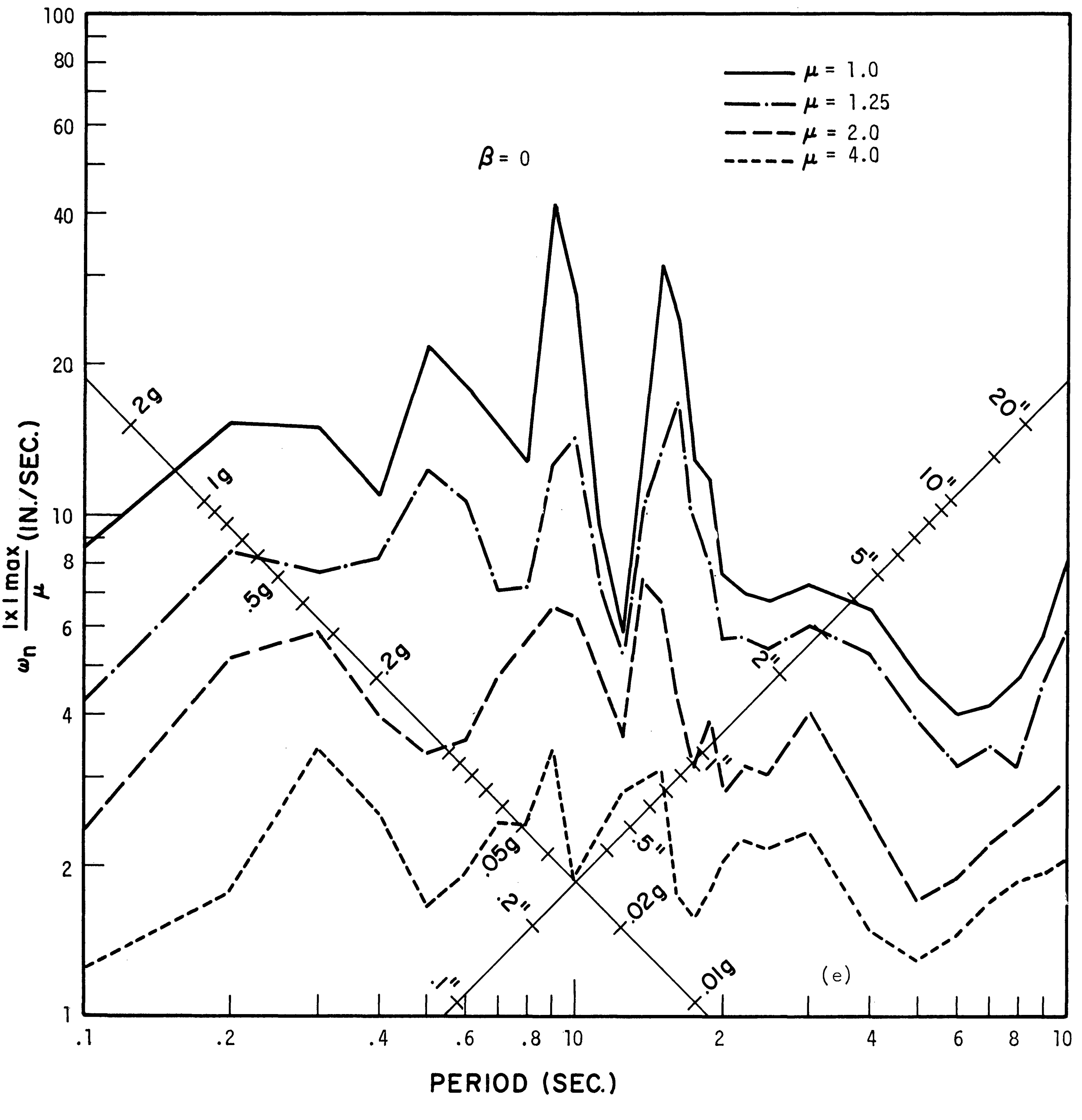

(b)

Figure 14. Continued.

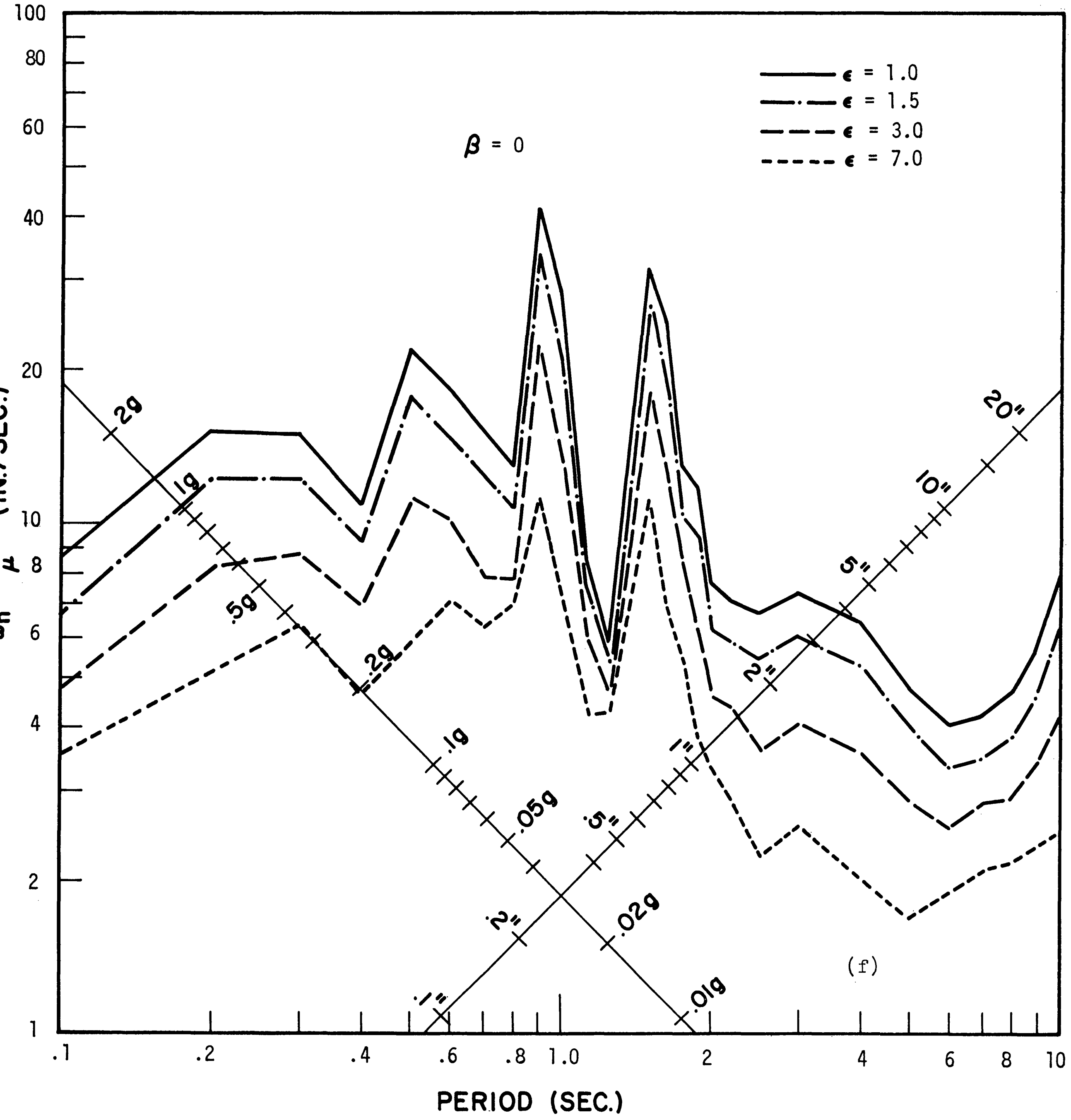

(a)

Figure 14. Response Spectra for the Elasto-Plastic System, Olympia, July 21, 1965, S86°W. Constant ductility ratio "μ".

SUMMARY AND CONCLUSIONS

In this report, the response of a Ramberg-Osgood type single-degree-of-freedom structure to strong-motion earthquake was studied. The principles and the construction of the response spectra were discussed. The discussion included force-displacement relation, equation of motion, response spectrum concepts, steady-state oscillation, and response spectra for strong-motion earthquakes. Also a family of spectral curves was presented for this system, where the Ramberg-Osgood exponent, restoring force amplitude, the ductility and the energy ratios were the main parameters considered.

From the results presented in this report the following conclusions can be drawn:

(1) The Ramberg-Osgood representation of the force-displacement relation is considered realistic if the structure is capable of maintaining stable, nondeteriorating hysteresis loops. Experimental work has produced remarkably stable hysteresis loops at large cyclic strains[4] which can be approximated closely by a Ramberg-Osgood function.

(2) For the steady-state vibration response, slowly varying parameter results showed good agreement with those of "downhill-climbing-method." The discrepancy between the two increased as exponent r and the ratio of input force to yield level of the system F_o/Q_y, became large. Neither result showed existence of unstable zone for the Ramberg-Osgood system.

(3) The spectral relation $|x|_{max} \approx |\dot{x}|_{max}/\omega_n \approx |\ddot{x} + \ddot{y}|_{max}/\omega_n^2$ is exact only for undamped linear systems, and is a good approximation for

damped linear systems provided the damping is small. The response spectra for linear systems are represented by the top curves of Figures 12 through 14. (The elasto-plastic system reduces to the elastic system when the ductility ratio μ or the energy ratio ϵ becomes equal to 1.)

(4) In nonlinear systems the spectral relation above is not valid. For the elasto-plastic systems this relation takes the form,

$$\frac{|x|_{max}}{\mu} \approx \frac{|\dot{x} + \dot{y}|_{max}}{\omega_n}$$

The expression on the left above, a pseudo velocity, is the quantity that was plotted to obtain the response spectra in this case.

(5) For Ramberg-Osgood systems there exists no simple spectral relation. It is noted however that in Ramberg-Osgood systems if V_d and V_a are defined as follows,

$$V_d \equiv \frac{\omega_n |x|_{max}}{\mu}, \text{ and } V_a \equiv \frac{|\ddot{x} + \ddot{y}|_{max}}{\omega_n}$$

then

$$V_d > V_a \quad \text{for} \quad \mu < 2$$

$$V_d = V_a \quad \text{for} \quad \mu = 2$$

$$V_d < V_a \quad \text{for} \quad \mu > 2$$

For values of ductility ratio less than two, the maximum difference between V_d and V_a occurs when μ equals one. It is also observed that the difference between the displacement and the acceleration spectrum curves for a given exponent r and constant ductility ratio is constant, and thus produces only a vertical shifting of the curves i.e. $V_d = k_s V_a$, where constant k_s is a function of μ and r . This does not apply to curves of constant energy ratio because the ductility ratio is no more constant. For the latter case $V_d \approx V_a$. Displacement and acceleration spectra for Ramberg-Osgood systems are plotted separately.

(6) It is noticed that in the Ramberg-Osgood system, the acceleration spectra is much more sensitive to changes in exponent r than is the displacement spectra which remained practically unchanged. The latter seems to point out the view that maximum displacement is independent of the degree of plasticity of the system.

(7) Taft and Olympia spectral curves are similar in form for constant ductility ratios, but not so similar for constant energy ratios. Taft spectral results for a given set of parameters are in general much greater, on the other hand, Olympia curves exhibited as a whole more fluctuation and sharper peaks.

(8) It is observed that inelastic action alone provides an important source of energy dissipation to damp out the response of a structure to an earthquake.

(9) The maximum displacement and the maximum energy input for Ramberg-Osgood systems are comparable with those obtained for elasto-plastic systems of the same period and yield level.

APPENDIX - NOTATION

The following symbols are used in this paper:

g	acceleration of gravity
k_s	a constant for Ramberg-Osgood spectra function of μ and r
m	mass
q	restoring force per unit mass = Q/m
q_y	yield or characteristic strength of spring per unit mass = Q_y/m
r	an exponent
t	time
x	relative displacement of mass to ground
x_o	extreme displacement of the restoring force
x_y	yield or characteristic displacement of spring
y	ground displacement
C_s	seismic lateral load coefficient
E_s	strain energy input
F_o	maximum amplitude of the forcing function
Q	restoring force
Q_y	yield or characteristic strength of spring
Q_o	Value of restoring force at reversal
V_a, V_d	maximum pseudo velocity
W	weight of the system
β	fraction of critical damping
ϵ	maximum strain energy input to recoverable strain energy at yield
ϵ_x	excursion ratio

μ	ductility ratio
τ	a time parameter
η	forcing frequency to undamped natural frequency
ϕ	a function of τ
Θ	$(\eta\tau + \phi)$
ω	frequency of input force
ω_n	undamped natural frequency of a system

NOTE: Differentiation with respect to time is denoted by dots.

REFERENCES

1. Goel, S. C. and Berg, G. V., "Inelastic Earthquake Response of Tall Steel Frames", ASCE Structural Engineering Conference, Seattle, Washington, May, 1967.

2. Alford, J. L., Housner, G. W., and Martel, R. R., "Spectrum Analyses of Strong-Motion Earthquakes," Earthquake Research Lab., California Inst. of Tech., August, 1951.

3. Jennings, P. C., "Response of Simple Yielding Structures to Earthquake Excitation," Ph.D. Thesis, Calif. Inst. of Tech., June, 1963.

4. Popov, E. P., Proceedings of Structural Engineers Association of California, 1965.

5. Kaldjian, M. J., "Moment-Curvature of Beams as Ramberg-Osgood Functions," Journal of the Structural Division, ASCE, Vol. 93, No. ST5, Proc. Paper 5488, October, 1967.

6. Jacobsen, L. S., "Frictional Effects in Composite Structures Subjected to Earthquake Vibrations," Report of the Dept. of Mechanical Engrg., Standford University, March, 1959.

7. Hanson, R. D., "Post-Elastic Dynamic Response of Mild Steel Structures," Ph.D. Thesis, California Institute of Technology, June, 1965.

8. Caughey, T. K., "Sinusoidal Excitation of a System with Bilinear Hysteresis," Journal of Applied Mechanics, Vol. 27, No. 4, December, 1960.

9. Blume, J. A., Newmark, N. M., and Corning, L. H., Design of Multistory Reinforced Concrete Buildings for Earthquake Motions, PCA, 1961.

10. Newmark, N. M. and Veletsos, A. S., "Effects of Inelastic Behavior on the Response of Systems," Proc. II World Conf. on Earthquake Engrg., Tokyo, Japan, July, 1960.

11. Berg, G. V. and Thomaides, S. S., "Punched Card Accelerogram of Strong-Motion Earthquakes," Univ. of Mich. Research Inst., Report No. 2881-1-P, September, 1959.